

Coastal vegetation and estuaries collectively reduce global warming

Judith A. Rosentreter^{1,2,3*}, Goulven G. Laruelle⁴, Hermann W. Bange⁵, Thomas S. Bianchi⁶, Julius J. M. Busecke⁷, Wei-Jun Cai⁸, Bradley D. Eyre³, Inke Forbrich^{9,10}, Eun YoungKwon¹¹, Taylor Maavara^{1,2}, Nils Moosdorf^{12,13,14}, Raymond G. Najjar¹⁵, V.V.S.S. Sarma¹⁶, Bryce Van Dam¹⁷, Pierre Regnier⁴

¹Yale Institute for Biospheric Studies, Yale University, New Haven, USA

²Yale School of the Environment, Yale University, New Haven, USA

³Center for Coastal Biogeochemistry, Faculty of Science and Engineering, Southern Cross University, Lismore, Australia

⁴Biogeochemistry and Modelling of the Earth System-BGEOSYS, Department of Geoscience, Environment and Society, Université Libre de Bruxelles, Brussels, Belgium

⁵Marine Biogeochemistry, Helmholtz Centre for Ocean Research Kiel, Kiel, Germany

⁶Department of Geological Sciences, University of Florida, Gainesville, USA

⁷Columbia University, Dept of Earth and Environmental Sciences, NY, USA

⁸School of Marine Science and Policy, University of Delaware, Newark, DE, USA

⁹Ecosystems Center, Marine Biological Laboratory, Woods Hole, USA

¹⁰Department of Environmental Sciences, University of Toledo, Toledo, USA

¹¹Center for Climate Physics, Institute for Basic Science, Busan, South Korea

¹²Leibniz Centre for Tropical Marine Research (ZMT), Bremen, Germany

¹³Kiel University, Kiel Germany

¹⁴Southern Cross Geoscience, Southern Cross University, Lismore, Australia

¹⁵Department of Meteorology and Atmospheric Science, The Pennsylvania State University, University Park, PA, USA

¹⁶CSIR-National Institute of Oceanography, 176 Lawsons Bay Colony, Visakhapatnam, India

¹⁷Department of Fluxes across interfaces, Institute of carbon cycles, Helmholtz-ZentrumHereon, Geesthacht, Germany

*email: judith.rosentreter@scu.edu.au

Abstract:

Coastal ecosystems release or absorb the greenhouse gases (GHG) carbon dioxide (CO₂), methane (CH₄), and nitrous oxide (N₂O) but the net effect of these ecosystems on global warming remains unknown. Here, we present a data-driven meta-analysis quantifying GHG fluxes in estuaries and coastal vegetation in ten world regions and globally. We show that the large GHG CO₂-equivalent (CO₂e) uptake by coastal vegetation is 23-28% offset by estuarine CO₂e outgassing, resulting in a global median [Q1-Q3] net sink of 389 [73-646] or 443 [173- 674] Tg CO₂e yr⁻¹ using the global warming potential for the 20-year or 100-year time horizon, respectively. We identify regional hotspot sinks in Southeast Asia, North America, and Africa. Globally, total coastal CH₄ and N₂O emissions offset 10-20% of the cooling effects of CO₂ uptake. Strengthening the coastal vegetation CO₂ sink while reducing the CH₄ and N₂O offsets will help mitigate global warming.

Keywords: Coastal vegetation, estuaries, climate change, greenhouse gas budget, global warming mitigation potential

Main

Since the beginning of the industrial era, atmospheric concentrations of CO₂, CH₄, and N₂O have increased by 47%, 156% and 23%, respectively, and continue to increase at alarming rates due to anthropogenic activities, driving global warming¹. While the global terrestrial CO₂ sink has significantly increased in the past decades², it is partially offset by associated CH₄ and N₂O emissions, resulting in a net GHG source to the atmosphere and a significant potential for global warming³. Globally, it is now clear that inland waters are atmospheric GHG source^{4,5} while the fluxes from coastal ecosystems are less certain. Located in the downstream portion of the Land-Ocean-Aquatic-Continuum (LOAC)⁶, estuaries receive large amounts of terrestrial carbon (C) and nitrogen (N) through riverine and groundwater flows, but their C and N cycles are also tightly inter-connected with coastal vegetated ecosystems⁷ and the coastal oceans^{8,9}. Net GHG fluxes from estuaries and coastal vegetation (mangroves, salt marshes, seagrasses) are thus a complex spatial and temporal combination of sources and sinks⁸, complicating estimates of their net effects to emphasize or mitigate global warming. A consistent global assessment of the GHG budget of the coastal zone is needed to implement efficient global warming mitigation strategies.

Estuaries and surrounding coastal vegetation are strongly interconnected but show remarkable variations in the magnitude and direction (sink or source) of GHG fluxes. Estuaries have been estimated to emit 0.4 to 2.2 Pg CO₂ yr⁻¹ globally⁸⁻¹¹, whereas mangroves and salt marshes collectively take up 0.3 to 1.7 Pg CO₂ yr⁻¹^{6,9} (*summarized in Supplementary Table S1*). Together with submergent seagrasses, coastal vegetation potentially store 304 (131-466) Tg CO₂ yr⁻¹ of so-called 'blue carbon' in their sediments^{12,13}. On the other hand, emissions of CH₄ and N₂O from coastal sediments and surrounding waters can offset some of the coastal vegetation carbon sinks^{14,15}, thereby complicating 'blue carbon' assessments^{16,17}. A recent global synthesis showed that median CH₄ emissions from combined mangrove, salt marshes, and seagrasses (0.52 Tg CH₄ yr⁻¹) exceed those from estuaries (0.23 Tg CH₄ yr⁻¹)¹⁸. However, CH₄ fluxes are highly variable across time and space, causing a large range in global estimates of both coastal vegetation (0.02 to 6.2 Tg CH₄ yr⁻¹)^{15,18} and estuaries (0.02 to 6.6 Tg CH₄ yr⁻¹)^{5,19} (*Supplementary Table S2*). Coastal N₂O fluxes are less understood and it remains unclear if coastal vegetated ecosystems are a net source or sink of N₂O to the atmosphere^{20,21}. Global estimates of estuarine N₂O emissions are highly uncertain, with large

discrepancies for both observation-based (110 to 2,844 Gg N₂O yr⁻¹)^{5,22,23} and modeling (94 to 1,084 Gg N₂O yr⁻¹)^{24,25} approaches (Supplementary Table S3).

Here we present a data-driven meta-analysis synthesizing CO₂, CH₄, and N₂O fluxes in three major estuary types (tidal systems and deltas, lagoons, and fjords) and three coastal vegetation types (mangroves, salt marshes, seagrasses), globally and in ten world regions. These regions were delineated by the REgional Carbon Cycle Assessment and Processes-2 (RECCAP2) project²⁶, an activity of the Global Carbon Project. We compiled water-air CO₂, CH₄, and N₂O fluxes for estuaries and combined CO₂ fluxes from eddy-covariance with CH₄ and N₂O fluxes from water-sediment-air interfaces for coastal vegetation. Our dataset compiles observations from a total of 738 sites from studies published between 1975 and 2020 and we provide a GHG flux climatology assumed representative for this period. The GHG fluxes are regionalized by combining GHG flux densities with recently published surface area distributions of coastal vegetation²⁷⁻²⁹ and estuaries³⁰. As such, our global-scale regional assessment applies a consistent framework for all three GHGs and ecosystems. Regional GHG fluxes are then summed to provide global net GHG fluxes for estuaries, coastal vegetation, and both systems combined. We quantify the net contemporary GHG balance in units of CO₂-equivalents (CO₂e) based on the global warming potential (GWP) of each gas for the 20 and 100 year time horizons¹. Following the RECCAP2 region segmentation, our coastal GHG budget can be integrated into broader budgets of continents.

Estuarine and coastal vegetation CO₂ fluxes

We estimate global median [first (Q1)-third (Q3) quartile] CO₂ emissions from estuaries at 111 [73-170] Tg CO₂ yr⁻¹ (Table 1), which is three to five times lower (as is our mean of 121 Tg CO₂ yr⁻¹) than recent mean estimates (370-550 Tg CO₂ yr⁻¹)^{10,11}. Our lower global emissions are due to the inclusion of estuarine surface area³⁰ (Figure 1) that is ~30% lower than previously estimated^{31,32}, and includes a greater number of sites than previous studies^{10,11}. In particular, CO₂ flux data in fjords have more than doubled since earlier reviews^{9,11} that considered fjords as minimal sources of atmospheric CO₂. Here we show that fjords take up 66 [24-96] Tg CO₂ yr⁻¹ from the atmosphere, thereby reducing 37% of the CO₂ emissions from global tidal systems and deltas (127 [90-176] Tg CO₂ yr⁻¹) and lagoons (50 [28-81] Tg CO₂ yr⁻¹) (Figure 2). Tidal systems and deltas which account for 40% of the global estuarine surface area (Supplementary Table S4) show higher CO₂ flux

densities than lagoon and fjords (Supplementary Table S5), likely due to their strong hydrological connectivity with rivers and groundwater that import CO₂ supersaturated waters³³. In addition, the relatively short residence times and the considerably strong influence by tides³¹ can increase water turbulence and therefore gas transfer velocities³⁴ which in turn enhance CO₂ evasion from tidal systems. At the regional scale, we find distinct trends of CO₂ fluxes between different geomorphic estuary types (Figure 2). For example, North America is a hotspot for atmospheric CO₂ uptake by fjords (57 [37-84] Tg CO₂ yr⁻¹, 86% of the CO₂ uptake by global fjords). Long stretches of lagoons can be found along Africa's coastline that contribute 24% to global lagoon CO₂ emissions. Europe accounts for 20% of global CO₂ emissions by tidal systems and deltas although only comprising 5% of the total surface area of this estuary type. This disproportionate contribution stems from the highest median CO₂ flux densities (4.7 g CO₂ m⁻² d⁻¹) of any estuary type or region (Supplementary Table S5), likely fuelled by organic carbon loads from European rivers under strong anthropogenic pressure³⁵. European estuaries were over-represented in previous global analyses^{10,11,36}, which likely led to overestimates in global CO₂ emissions from estuaries.

Using data exclusively from eddy-covariance long-term studies, we estimate that salt marshes, mangroves, and seagrasses worldwide take up 601 [426-774] Tg CO₂ yr⁻¹ from the atmosphere, a flux which, in absolute terms, is more than five times greater than the estuarine CO₂ outgassing (Table 1). Our global estimate is lower but within the uncertainty range of a recent estimate of 843±440 Tg CO₂ yr⁻¹ by mangroves, salt marshes, and seagrasses⁶. Seagrass meadows can be found in tropical, subtropical, and temperate-cold climate zones and are abundant across different climates. Mangroves are abundant in subtropical and tropical climates, whereas salt marshes dominate in temperate regions (Figure 1, Supplementary Figure S1). As expected, highly productive mangrove forests that consist of large carbon stocks³⁷ contribute the majority (60%) of the global CO₂ uptake by coastal vegetation (359 [333-434] Tg CO₂ yr⁻¹). Globally, seagrasses (192 [53-354] Tg CO₂ yr⁻¹) have a ~4 times higher CO₂ uptake than salt marshes (50 [41-59] Tg CO₂ yr⁻¹), which is similar to previous findings based on net primary (or ecosystem) production^{38,39}. Since mangrove forests are abundant in tropical southeast Asia (Figure 1), we find that this region contributes most (37%) to global mangrove CO₂ uptake, followed by Africa (20%), and tropical North and South America (both ~15%). Salt marshes are abundant along the west and east coasts of Canada and the US. Therefore, North America

contributes to most of the global CO₂ uptake by salt marshes (34%). Other regions that provide a substantial salt marsh CO₂ sink include East Asia (23%) and Australasia(21%). Africa’s coastline has the greatest contribution (24%) to global seagrass CO₂ uptake.

Figure 1

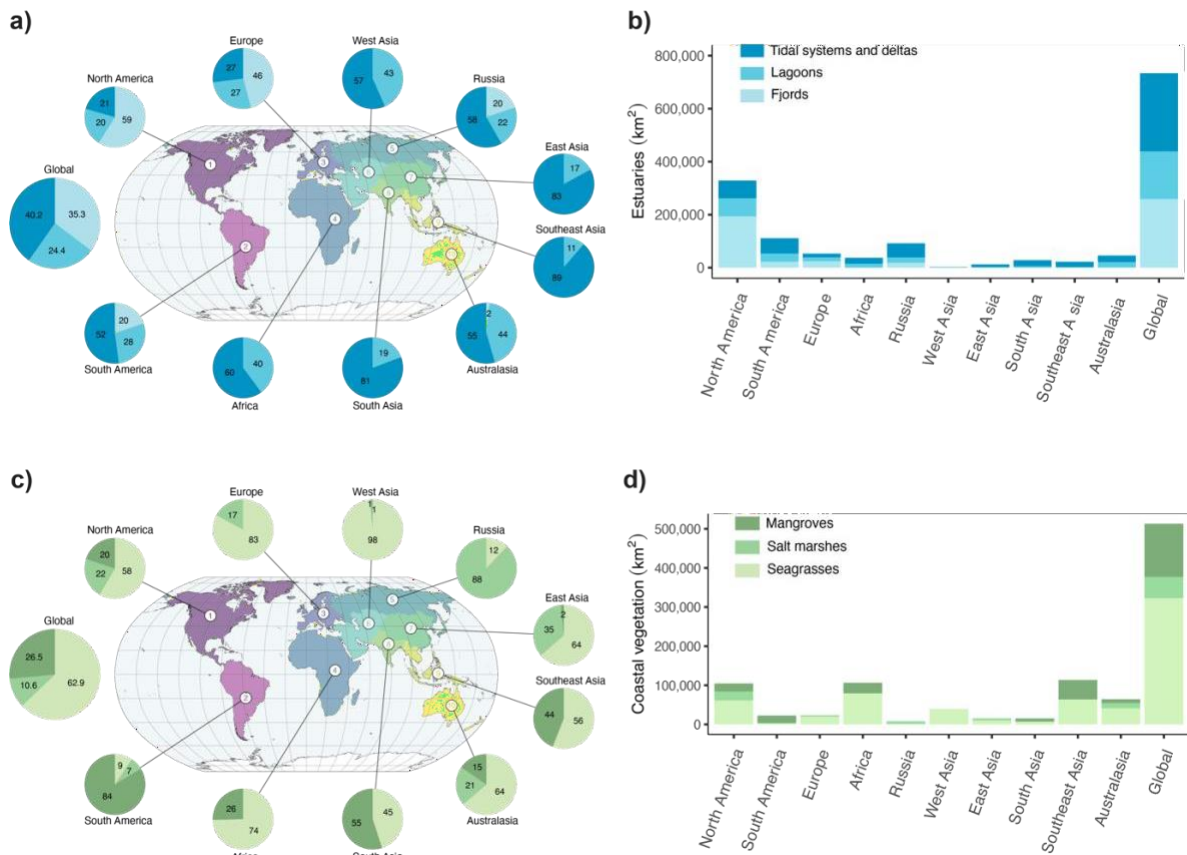
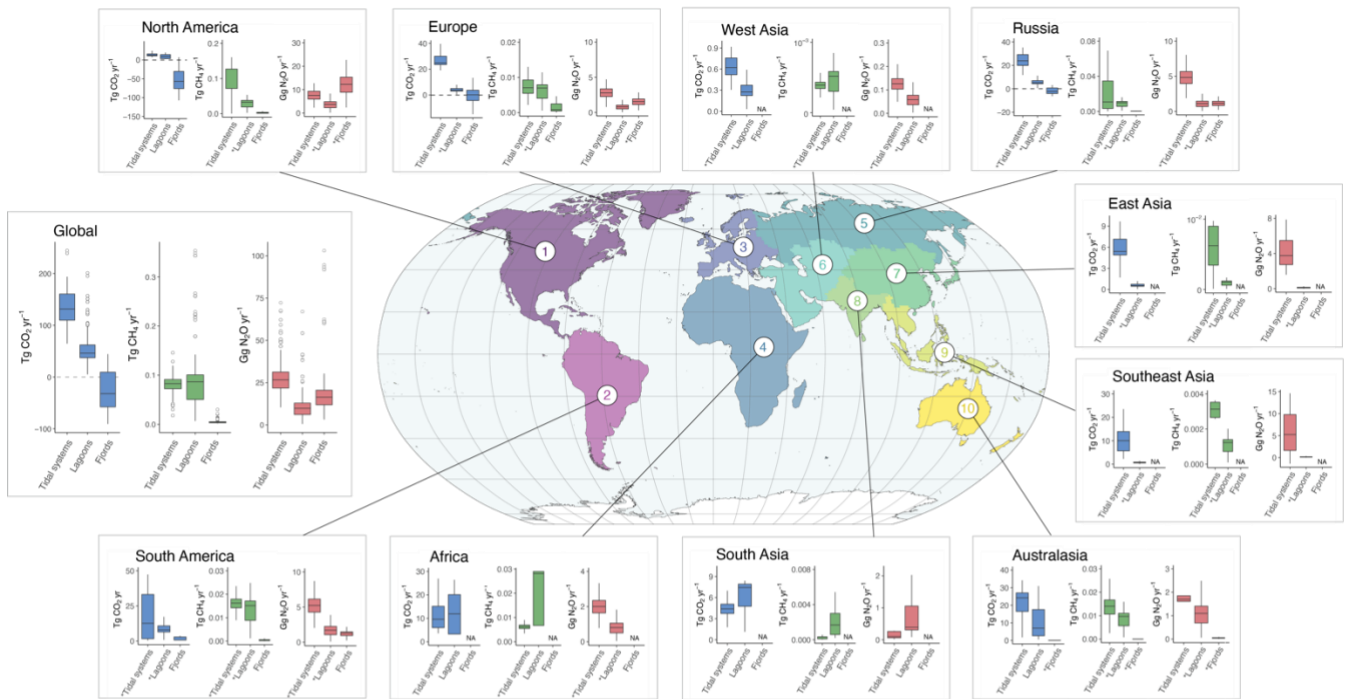


Figure 1 caption: Regional and global surface areas of estuaries and coastal vegetation. Surface areas of estuaries a) as a relative percentage (%) and b) in km² of tidal systems and deltas, lagoons, and fjords in the ten RECCAP2 world regions and globally. Surface areas of coastal vegetation c) as a relative percentage (%) and d) in km² of mangroves, salt marshes, and seagrasses in the ten RECCAP2 world regions and globally. The global surface area for estuaries is 733,801 km² ³⁰. The global coastal vegetation area is 512,982 km². Surface areas (km²) for each estuary and coastal vegetation type in each of the ten regions can be found in Supplementary Table S4.

Figure 2

a)



b)

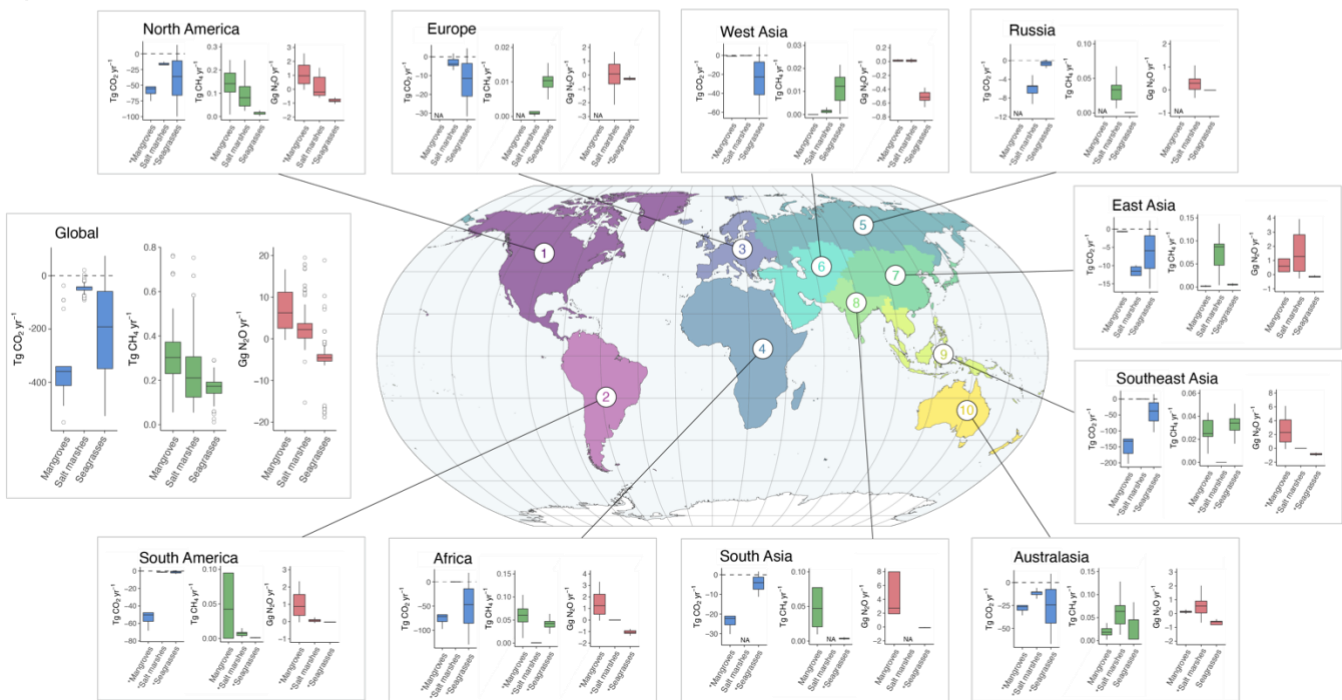


Figure 2 caption: Regional and global estuary and coastal vegetation GHG fluxes. The box- whisker plots show the median and interquartile (Q1-Q3) range of CO₂, CH₄, and N₂O fluxes yr⁻¹ in a) estuaries (tidal systems and small deltas, lagoons, fjords); and b) coastal vegetation (mangroves, salt marshes, seagrasses) in ten RECCAP2 regions and globally. A positive value indicates a flux from the ecosystem to the atmosphere and a negative value a flux from the atmosphere to the ecosystem. Outliers (open circles) are shown only for global plots. The asterisk (*) indicates that the flux was upscaled based on global statistics (n < 3) (see Methods).

Estuarine and coastal vegetation CH₄ fluxes

Global estuaries emit 0.25 [0.07-0.46] Tg CH₄ yr⁻¹ (Table 1), a median value that falls at the lower end of the range of previously reported values^{5,19,40} (Supplementary Table S2), yet is close to the recent median estimate (0.23 [0.02-0.91] Tg CH₄ yr⁻¹) by Rosentreter et al.¹⁸, which did not explore regional and estuary-type contributions. Global estuarine CH₄ emissions are dominated by tidal systems and deltas (0.14 [0.11-0.23] Tg CH₄ yr⁻¹, 56%), followed by lagoons (0.11 [0.05-0.13] Tg CH₄ yr⁻¹, 44%), while the contribution from fjords is negligible (<1%). Our regional analysis shows that North America's tidal systems and deltas contribute the majority (28%) of global CH₄ emissions from this estuary type (Figure 2). North America also has the highest median CH₄ flux densities (2.9 mg CH₄ m⁻² d⁻¹) of tidal systems and deltas, particularly in the USA, where many eutrophic systems undergo seasonal hypoxia or anoxia that fuel CH₄ production⁴¹. South America, Russia, and Australasia contribute around 10% each to global CH₄ emissions from tidal systems and deltas, whereas all other regions are minor contributors (< 5%). North America comprises the largest area of lagoons (Figure 1), thereby dominating global lagoonal CH₄ emissions (30%). Other regions with substantial lagoon CH₄ emissions are Africa (25%) and South America (14%), whereas the remaining regions contribute <10%. Interestingly, we find that of all estuary types and regions, lagoons in Africa show the highest flux density (5.3 mg CH₄ m⁻² d⁻¹), driven by high CH₄ production in anoxic bottom waters in permanently stratified lagoons along the Ivory Coast⁴².

Globally, mangroves, salt marshes, and seagrasses combined release 0.76 [0.47-1.41] Tg CH₄ yr⁻¹ which is more than three times the CH₄ released by global estuaries. Our coastal vegetation estimate is comparable with a recent review¹⁸ but incorporates more data, which results in an increased estimate for salt marshes and mangroves but not seagrasses. We find that mangroves (0.34 [0.21-0.50] Tg CH₄ yr⁻¹) dominate coastal vegetation CH₄ emissions, followed by salt marshes (0.26 [0.14-0.36] Tg CH₄ yr⁻¹), and seagrasses (0.17 [0.09-0.21] Tg CH₄ yr⁻¹) (Table 1). The relatively high CH₄ emissions from mangroves (exceeding global estuaries) are promoted by carbon-rich deep anoxic sediments⁴³ and by tidally induced mixing between groundwater rich in CH₄ and surface waters⁴⁴. While the highest mangrove CH₄ flux densities (21 mg CH₄ m⁻² d⁻¹) are in East Asia, North America's mangrove forests dominate (42%) global mangrove CH₄ emissions. This is because its forest area is 86 times greater than in East Asia, and the CH₄ flux density is still high (18 mg CH₄ m⁻² d⁻¹) (Supplementary Table S6). While Southeast Asia dominates mangrove forest area globally, the region's much lower CH₄ flux density (1.4 mg CH₄ m⁻² d⁻¹) means that it adds only 7% to global mangrove CH₄ emissions.

Such a low regional evasion rate may be explained by high monsoonal rainfall events and short water residence times, resulting in low rates of organic matter decomposition⁴⁵. The highest median CH₄ flux densities of any coastal vegetation type are found in East Asian salt marshes (44 mg CH₄ m⁻² d⁻¹), contributing 34% of global salt marsh CH₄ emissions despite its relatively small marsh coverage. North America's vast salt marsh areas are the second highest contributor (32%) to global salt marsh emissions. Australasia's seagrass meadows dominate (26%) global seagrass CH₄ emissions, a combination of moderately high seagrass area and a regional flux density that is more than twice the global median (Supplementary Table S6).

Estuarine and coastal vegetation N₂O fluxes

We estimate that estuaries globally emit 61 [41-94] Gg N₂O yr⁻¹ (Table 1), which is substantially lower than previous observational and modeling estimates (94 to 5,710 Gg N₂O yr⁻¹)^{5,24,25,46} (Supplementary Table S3). Similar to CO₂ and CH₄, our lower estuary N₂O emissions are partially due to lower estuarine surface area used in this study³⁰, but also reflects the ~80% more sites in our analysis than earlier reviews^{23,46}. We find the highest N₂O emissions are from tidal systems and deltas (35 [24-48] Gg N₂O yr⁻¹), but in contrast to CO₂ and CH₄, fjords have the second highest N₂O emissions (16 [12-21] Gg N₂O yr⁻¹), almost double of those of lagoons (10 [6-14] Gg N₂O yr⁻¹). A comparison of the ten regions shows that North America contributes 27%, 15%, and 77% to global emissions from tidal systems and deltas, lagoons, and fjords, respectively, resulting in 25 [17-33] Gg N₂O yr⁻¹ (40%) contribution to global estuary N₂O emissions (Figure 2). Other regions of moderate contributions are South America (14%), Russia (12%), and Southeast Asia (9%), with the remaining regions being only minor contributors (< 5 Gg N₂O yr⁻¹). We further compare our data-driven approach with the recently published mechanistic model of global estuary N₂O emissions²⁵ that was regionalised for the purpose of comparison to this study. The modelled global emissions estimates from all three estuary types (94 Gg N₂O yr⁻¹) are consistent with the upper uncertainty bound of those calculated with the data-driven approach. As such, we find an overall good agreement between the two approaches. Fjord estimates represent the largest relative difference between modelled and data-driven estimates (Table 1).

Coastal vegetation can be sources or sinks of N₂O to the atmosphere. We find that emissions slightly exceed uptake at the global scale, resulting in 6.3 [0.7-18.3] Gg N₂O yr⁻¹ which is only about 10% of the estuarine emission (Table 1). Globally, mangroves emit 8.9 [4.4-19.3] Gg N₂O yr⁻¹, at least four times more N₂O than salt marshes (2.1 [-0.8-6.1] Gg N₂O yr⁻¹).

Seagrasses take up 4.6 [3.4-6.0] Gg N₂O yr⁻¹, thereby offsetting almost half of the N₂O emitted by salt marshes and mangroves. Nevertheless, large variability can be found in local N₂O measurements in coastal vegetation. For example, current studies report N₂O uptake from salt marshes in North America⁴⁷ and Europe⁴⁸, while studies from East Asia, mainly China, reveal that this region accounts for a substantial 1.3 [0.2-2.8] Gg N₂O yr⁻¹ (61%) of global salt marsh emissions. Mangroves ecosystems are generally a source of N₂O although some mangrove creeks in Australia have been shown to consume N₂O due to low nitrogen concentrations^{20,21}. Our seagrass N₂O flux database is strongly biased towards data from Australia, where studies mostly suggest N₂O uptake from near-pristine seagrasses⁴⁹ (Supplementary Table S7).

Figure 3

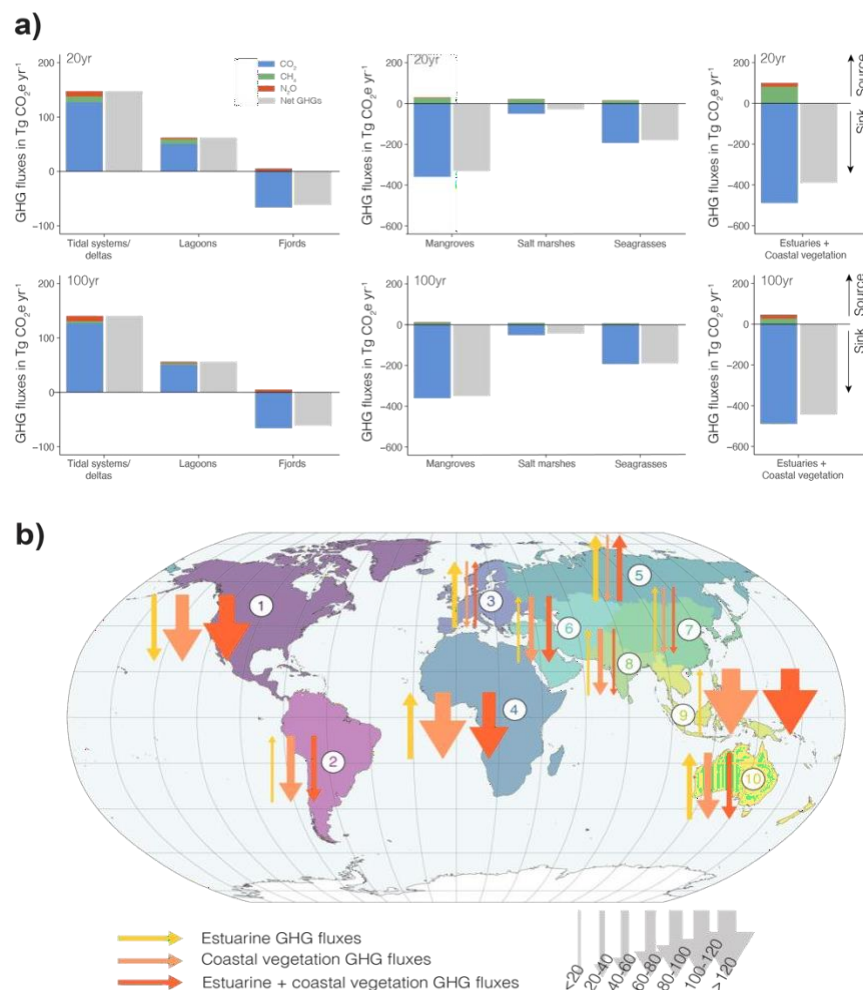
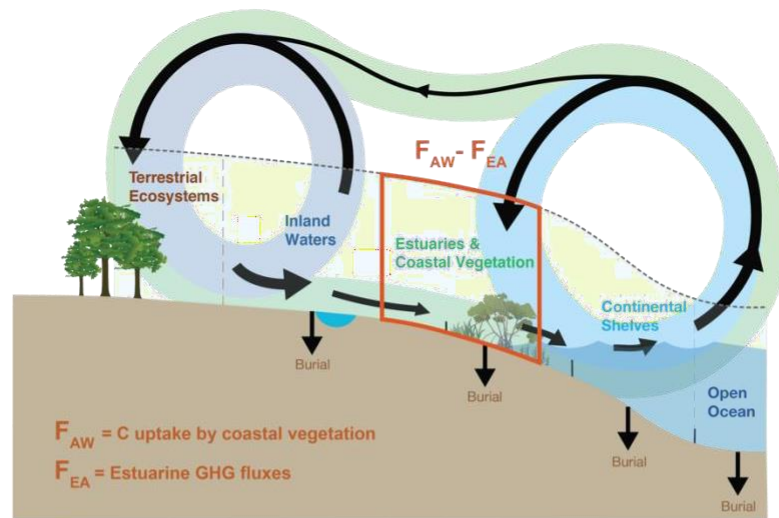


Figure 3 caption: Global and regional coastal CO₂-equivalent GHG fluxes.

a) Global median GHG sources and sinks of estuaries and coastal vegetation using the 20-year (top) and 100-year (bottom) time horizons. The warming /cooling potential is expressed as CO₂-equivalents in Tg CO₂e yr⁻¹ for CO₂, CH₄, N₂O, and their sum (net GHGs). b) Conceptual diagram showing the magnitude of the CO₂-equivalent GHG fluxes for estuaries, coastal vegetation, and their sum in the ten RECCAP2 regions and relative to each other. The size of the arrows is proportional to the fluxes in Tg CO₂e yr⁻¹ (Table 2). The arrow size is the same for GWP₂₀ and GWP₁₀₀, therefore arrows are not shown for the two GWP time horizons individually.

Figure 4

a)



b)

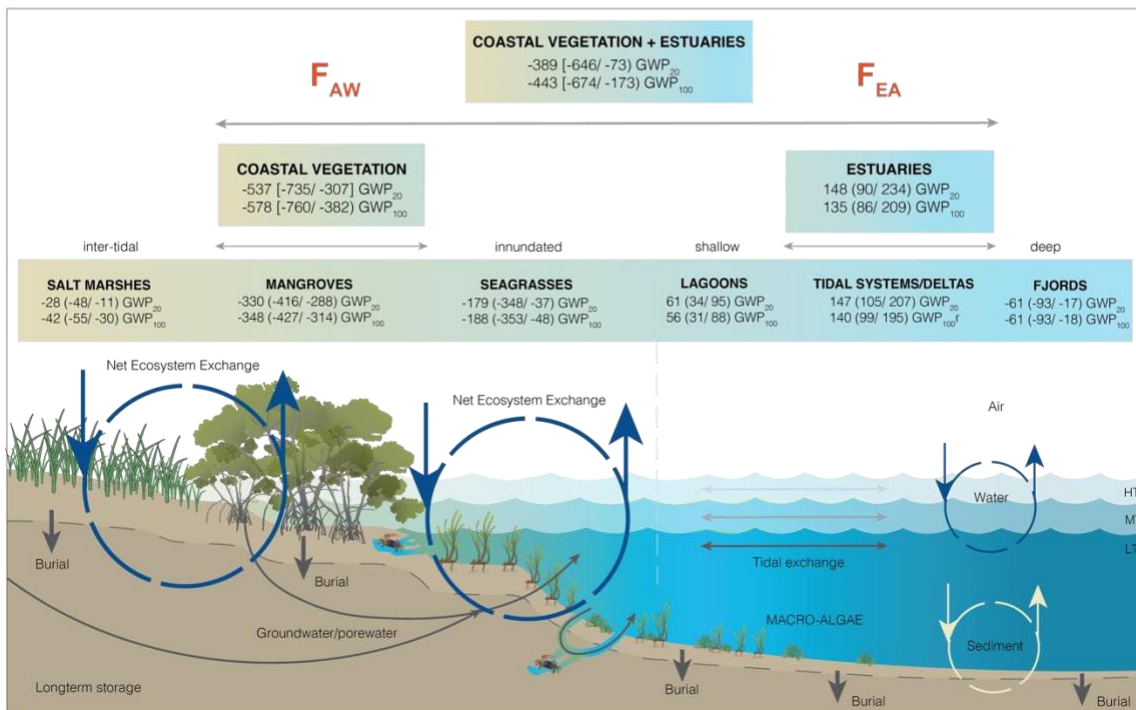


Figure 4 caption: Estuary and coastal vegetation GHG fluxes in the land-to-ocean aquatic continuum (LOAC). a) the LOAC carbon loop model adapted from Regnier et al.⁶. The green loop connects the terra-firme ecosystems to the open ocean. The two shorter loops connect the terra firme ecosystems to inland waters (grey) and the coastal vegetation, estuaries, and continental shelves to the open ocean (blue). F_{AW} refers to CO_2 uptake by tidal wetlands (salt marshes and mangroves) and submerged vegetation and F_{EA} refers to estuarine outgassing. b) Global median [Q1/Q3] CO_2 -equivalent GHG fluxes using the global warming potential (GWP) for the 20-year and 100-year time horizons in coastal vegetation and in estuaries. Here we include seagrasses in coastal vegetation fluxes (F_{AW}), whereas in Regnier et al.⁶ seagrasses and macro-algae as submerged vegetation are separated from inter-tidal emergent mangroves and salt marshes. Units are in $Tg\ CO_2e\ yr^{-1}$.

Implication for regional and global budgets

Our data-driven meta-analysis reveals that estuarine CO₂-equivalent GHG emissions offset the coastal vegetation CO₂-equivalent GHG uptake, by 28% for the GWP₂₀ and 23% for the GWP₁₀₀. Estuaries and coastal vegetation therefore have a global net cooling effect, corresponding to a GHG sink for the atmosphere of 389 [73-646] Tg CO₂e yr⁻¹ and 443 [173-674] Tg CO₂e yr⁻¹ based on GWP₂₀ and GWP₁₀₀, respectively (Figure 3). Our quantification of the net GHG sink is broadly consistent with previous assessments based solely on CO₂^{6,8,9}. However, we find that this sink results both from a downward revision of coastal vegetation CO₂ fixation and a significantly lower estuarine GHG outgassing, mostly due to the CO₂ uptake by fjords and a reduced estuarine surface area³⁰. The net CO₂ sink of estuaries and coastal vegetation is also significantly compensated by CH₄ and N₂O emissions, which offset 21% for the GWP₂₀ and 10% for the GWP₁₀₀. Our global-scale assessment, using the largest dataset so far, significantly reduces the uncertainty in the contemporary GHG budget⁶ and emphasises the global cooling effects of coastal vegetation and estuaries combined, in contrast to terrestrial sources³ and inland waters^{4,5} (Figure 4). Importantly, we reveal where estuarine fluxes enhance, partially offset, or exceed coastal vegetation CO₂ uptake, allowing us to identify regional hotspots of GHG uptake and release (Figure 3). We find that 8 out of 10 coastal regions are a net GHG sink for the atmosphere, regardless of the time horizon considered (Table 2). Using the GWP₁₀₀, Southeast Asia shows the greatest net GHG sink (156 [106-224] Tg CO₂e yr⁻¹) because of its extensive and highly productive tropical mangrove forests and seagrass meadows (Figure 1), as well as having relatively few estuaries compared to other regions³⁰. A second regional hotspot for GHG sinks is North America (127 [76-165] Tg CO₂e yr⁻¹) due to its expansive mangrove, salt marsh, and seagrass areas, while also having the largest area of CO₂-absorbing fjords globally (40% of which are located in Greenland). In Africa, the large CO₂ uptake by coastal vegetation is partially offset by estuarine GHG outgassing, leaving Africa as the third greatest net GHG sink (93 [35-134] Tg CO₂e yr⁻¹), globally. Australasia and West Asia are moderate GHG sinks (~25 Tg CO₂e yr⁻¹), whereas in East and South Asia, coastal vegetation CO₂ sinks are largely offset by estuarine GHG release, resulting in a small net GHG sink of <12 Tg CO₂e yr⁻¹. In Europe and Russia, estuarine GHG outgassing across a large estuarine surface area exceeds uptake from the relatively small area of coastal vegetation, making these regions net GHG sources. As such, our regionalized assessment suggests that in addition to being a net global sink of GHGs for the atmosphere, the sink attributed to estuaries and coastal vegetation is also a common feature in many regions across the world.

Our coastal GHG synthesis, which is the first to combine coastal vegetation and estuaries and to combine the three major GHGs, also affords the opportunity to identify limitations and recommend areas most in need of research. The limitations fall largely into three categories: mapping of ecosystems, GHG flux measurements, and spatio-temporal variability. The most notable gap is for macroalgae, which have not been mapped globally and are greatly lacking in flux measurements, despite their large potential for carbon sequestration⁵⁰. Marsh area is likely underestimated, given a very recent analysis⁵¹ and the lack of global mapping of freshwater tidal marshes. GHG flux measurements, despite recent progress, are still lacking, particularly from Africa, Russia, and West Asia. In all regions, seagrass GHG (and particularly N₂O) flux studies are rare. Coastal ecosystems have high temporal variability, therefore more eddy covariance towers, and conventional time-series measurements are needed, even in regions with good spatial coverage. High spatio-temporal variability means that techniques such as remote sensing⁵¹, empirical modeling, and process-based modeling are needed for extrapolating flux densities and projecting future areas and flux densities, particularly in the face of climate change and population growth along the coast. Despite its limitations, our regional coastal GHG synthesis addresses the current research gap between local and global scales. The substantial coastal carbon sink value of US\$ 20 billion (US\$50 per ton carbon) highlights the urgency to protect the coastal zone from development, hydrological alterations, and climate change impacts such as sea level rise.

Acknowledgments

We would like to thank the RECCAP2 Scientific Committee and the Global Carbon Project that initiated this group effort: <https://www.globalcarbonproject.org/reccap/index.htm>. JAR and TM acknowledge funding by the Hutchinson Postdoctoral Fellowship from the Yale Institute for Biospheric Studies at Yale University. IF acknowledges the NSF LTER program (OCE 1637630). RGN acknowledges support from NASA's Carbon Cycle Science Program. GGL is research associate of the F.R.S-FNRS at the Université Libre de Bruxelles. PR received financial support from BELSPO through the project ReCAP, which is part of the Belgian research program FedTwin, and from the European Union's Horizon 2020 research and innovation program ESM 2025 – Earth System Models for the Future (grant no. 101003536) project. BDE acknowledges support from ARC grants DP220100918, LP200200910 and LP190100271.

Data availability

The datasets that support the findings of this study are available in the Figshare repository:

References

1. IPCC, I. *Climate Change 2021: The Physical Science Basis. Contribution of Working Group I to the Sixth Assessment Report of the Intergovernmental Panel on Climate Change* (2021).
2. Friedlingstein, P., Sullivan, M. O., Jones, M. W., Andrew, R. M. & Hauck, J. Data description paper Global Carbon Budget 2020. *Earth Syst. Sci. Data* **2020**, 3269–3340 (2020).
3. Tian, H. *et al.* The terrestrial biosphere as a net source of greenhouse gases to the atmosphere. *Nature* **531**, 225–228 (2016).
4. Raymond, P. A. *et al.* Global carbon dioxide emissions from inland waters. *Nature* **503**, 355–359 (2013).
5. Zheng, Y. *et al.* Global methane and nitrous oxide emissions from inland waters and estuaries. *Glob. Chang. Biol.* 4713–4725 (2022).
6. Regnier, P., Resplandy, L., Najjar, R. G. & Ciais, P. The land-to-ocean loops of the global carbon cycle. *Nature* **603**, 401–410 (2022).
7. Abril, G. & Borges, A. V. Ideas and perspectives: Carbon leaks from flooded land: Do we need to replumb the inland water active pipe? *Biogeosciences* **16**, 769–784 (2019).
8. Cai, W.-J. Estuarine and Coastal Ocean Carbon Paradox: CO₂ Sinks or Sites of Terrestrial Carbon Incineration? *Ann. Rev. Mar. Sci.* **3**, 123–145 (2011).
9. Bauer, J. E. *et al.* The changing carbon cycle of the coastal ocean. *Nature* **504**, 61–70 (2013).
10. Chen, C. T. A. *et al.* Air-sea exchanges of CO₂ in the world’s coastal seas. *Biogeosciences* **10**, 6509–6544 (2013).
11. Laruelle, G. G. *et al.* Global multi-scale segmentation of continental and coastal waters from the watersheds to the continental margins. *Hydrol. Earth Syst. Sci.* **17**, 2029–2051 (2013).
12. Macreadie, P. I. *et al.* Blue carbon as a natural climate solution. *Nat. Rev. Earth Environ.* **0123456789**, (2021).
13. Gattuso, J.-P., Williamson, P., Duarte, C. M. & Magnan, A. K. The Potential for Ocean-Based Climate Action: Negative Emissions Technologies and Beyond. *Front. Clim.* **2**, 1–8 (2021).
14. Rosentreter, J. A., Maher, D. T., Erler, D. V, Murray, R. H. & Eyre, B. D. Methane emissions partially offset “blue carbon” burial in mangroves. *Sci. Adv.* **4**, eaao4985 (2018).
15. Al-Haj, A. N. & Fulweiler, R. W. A synthesis of methane emissions from shallow vegetated coastal ecosystems. *Glob. Chang. Biol.* **26**, 2988–3005 (2020).
16. Rosentreter, J. A., Al-Haj, A. N., Fulweiler, R. W. & Williamson, P. Methane and Nitrous Oxide Emissions Complicate Coastal Blue Carbon Assessments. *Global Biogeochem. Cycles* **35**, 1–8 (2021).
17. Williamson, P. & Gattuso, J. Carbon Removal Using Coastal Blue Carbon Ecosystems Is Uncertain and Unreliable, With Questionable Climatic Cost-Effectiveness. *Front. Clim.* **4**, 1–14 (2022).

18. Rosentreter, J. A. *et al.* Half of global methane emissions come from highly variable aquatic ecosystem sources. *Nat. Geosci.* **14**, 225–230 (2021).
19. Borges, A. V. & Abril, G. Carbon Dioxide and Methane Dynamics in Estuaries. in *Treatise on Estuarine and Coastal Science* vol. 5 119–161 (Elsevier, 2011).
20. Maher, D. T., Sippo, J. Z., Tait, D. R., Holloway, C. & Santos, I. R. Pristine mangrove creek waters are a sink of nitrous oxide. *Sci. Rep.* **6**, 25701 (2016).
21. Murray, R., Erler, D., Rosentreter, J., Maher, D. & Eyre, B. A seasonal source and sink of nitrous oxide in mangroves: Insights from concentration, isotope, and isotopomer measurements. *Geochim. Cosmochim. Acta* **238**, (2018).
22. De Wilde, H. P. J. & De Bie, M. J. M. Nitrous oxide in the Schelde estuary: Production by nitrification and emission to the atmosphere. *Mar. Chem.* **69**, 203–216 (2000).
23. Murray, R. H., Erler, D. V. & Eyre, B. D. Nitrous oxide fluxes in estuarine environments: response to global change. *Glob. Chang. Biol.* **21**, 3219–3245 (2015).
24. Kroeze, C., Dumont, E. & Seitzinger, S. Future trends in emissions of N₂O from rivers and estuaries. *J. Integr. Environ. Sci.* **7**, 71–78 (2010).
25. Maavara, T. *et al.* Nitrous oxide emissions from inland waters: Are IPCC estimates too high? *Glob. Chang. Biol.* **25**, 473–488 (2019).
26. Ciais, P. *et al.* Definitions and methods to estimate regional land carbon fluxes for the second phase of the REgional Carbon Cycle Assessment and Processes Project (RECCAP-2). *Geosci. Model Dev. Discuss.* **2020**, 1–46 (2020).
27. Bunting, P. *et al.* The Global Mangrove Watch - A New 2010 Global Baseline of Mangrove Extent. *Remote Sens.* **10**, 1669 (2018).
28. Mcowen, C. *et al.* A global map of saltmarshes. *Biodivers. Data J.* **5**, e11764 (2017).
29. UNEP-WCMC, Short FT (2017). Global distribution of seagrasses (version 6.0). Sixth update to the data layer used in Green and Short (2003). Cambridge (UK): UN Environment World Conservation Monitoring Centre. URL: <http://data.unepwcmc.org/datasets/7>
30. Laruelle, G. G., Rosentreter, J. A., Regnier P. Extrapolation based regionalized re-evaluation of the global estuarine surface area. (in prep.).
31. Dürr, H. H. *et al.* Worldwide typology of nearshore coastal systems: defining the estuarine filter of river inputs to the oceans. *Estuaries and Coasts* **34**, 441–458 (2011).
32. Woodwell, G. M., Rich, P. H. & Hall, C. A. S. Carbon in estuaries. in *Carbon and the Biosphere* (eds. Woodwell, G. M. & Pecan, E. V) 221–240 (Technical Information Center, U.S. Atomic Energy Commission, National Technical Information Service, 1973).
33. Stewart, B. T., Santos, I. R., Tait, D. R., Macklin, P. A. & Maher, D. T. Submarine groundwater discharge and associated fluxes of alkalinity and dissolved carbon into Moreton Bay (Australia) estimated via radium isotopes. *Mar. Chem.* **174**, 1–12 (2015).
34. Borges, A. V. *et al.* Variability of the gas transfer velocity of CO₂ in a macrotidal estuary (the Scheldt). *Estuaries* **27**, 593–603 (2004).

35. Frankignoulle, M. Carbon Dioxide Emission from European Estuaries. *Science* **282**, 434–436 (1998).
36. Regnier, P. *et al.* Modelling Estuarine Biogeochemical Dynamics: From the Local to the Global Scale. *Aquat. Geochemistry* **19**, 591–626 (2013).
37. Alongi, D. M. Carbon Cycling and Storage in Mangrove Forests. *Ann. Rev. Mar. Sci.* **6**, 195–219 (2014).
38. Alongi, D. M. Carbon Balance in Salt Marsh and Mangrove Ecosystems: A Global Synthesis. *J. Mar. Sci. Eng.* **8**, 767 (2020).
39. Duarte, C. M. Reviews and syntheses: Hidden forests, the role of vegetated coastal habitats in the ocean carbon budget. *Biogeosciences* **14**, 301–310 (2017).
40. Bange, H. W., Bartell, U. H., Rapsomanikis, S. & Andreae, M. O. Methane in the Baltic and North Seas and a reassessment of the marine emissions of methane. *Global Biogeochem. Cycles* **8**, 465–480 (1994).
41. Gelesh, L., Marshall, K., Boicourt, W. & Lapham, L. Methane concentrations increase in bottom waters during summertime anoxia in the highly eutrophic estuary, Chesapeake Bay, U.S.A. *Limnol. Oceanogr.* **61**, S253–S266 (2016).
42. Koné, Y. J. M., Abril, G., Delille, B. & Borges, A. V. Seasonal variability of methane in the rivers and lagoons of Ivory Coast (West Africa). *Biogeochemistry* **100**, 21–37 (2010).
43. Donato, D. C. *et al.* Mangroves among the most carbon-rich forests in the tropics. *Nat. Geosci.* **4**, 293–297 (2011).
44. Maher, D. T., Santos, I. R., Golsby-Smith, L., Gleeson, J. & Eyre, B. D. Groundwater-derived dissolved inorganic and organic carbon exports from a mangrove tidal creek: The missing mangrove carbon sink? *Limnol. Oceanogr.* **58**, 475–488 (2013).
45. Rao, G. D. & Sarma, V. V. S. S. Variability in Concentrations and Fluxes of Methane in the Indian Estuaries. *Estuaries and Coasts* **39**, 1639–1650 (2016).
46. Bange, H. W., Rapsomanikis, S. & Andreae, M. O. The Aegean Sea as a source of atmospheric nitrous oxide and methane. *Mar. Chem.* **53**, 41–49 (1996).
47. Chmura, G. L., Kellman, L., van Ardenne, L. & Guntenspergen, G. R. Greenhouse Gas Fluxes from Salt Marshes Exposed to Chronic Nutrient Enrichment. *PLoS One* **11**, e0149937 (2016).
48. Dausse, A. *et al.* Biogeochemical functioning of grazed estuarine tidal marshes along a salinity gradient. *Estuar. Coast. Shelf Sci.* **100**, 83–92 (2012).
49. Chen, J., Wells, N. S., Erler, D. V. & Eyre, B. D. Land-Use Intensity Increases Benthic N₂O Emissions Across Three Sub-Tropical Estuaries. *J. Geophys. Res. Biogeosciences* **127**, 1–15 (2022).
50. Krause-Jensen, D. & Duarte, C. M. Substantial role of macroalgae in marine carbon sequestration. *Nat. Geosci.* **9**, 737–742 (2016).
51. Murray, N. J. *et al.* High-resolution mapping of losses and gains of Earth's tidal wetlands. *Science* **376**, 744–749 (2022).

Table 1: Global coastal vegetation and estuaries greenhouse gas fluxes.Global median [Q1-Q3] CO₂, CH₄, N₂O, and CO₂-equivalent (CO₂e) fluxes using the GWP₂₀ and GWP₁₀₀.

	CO ₂ (Tg CO ₂ yr ⁻¹)	CH ₄ (Tg CH ₄ yr ⁻¹)	CH ₄ (Tg CO ₂ e yr ⁻¹)(20yr)	CH ₄ (Tg CO ₂ e yr ⁻¹)(100yr)	N ₂ O (Gg N ₂ O yr ⁻¹)	N ₂ O (Tg CO ₂ e yr ⁻¹)(20yr, 100yr) ^a
Tidal systems and deltas	127 [90-176]	0.14 [0.11-0.23]	11.00 [8.83-18.42]	3.78 [3.03-6.33]	35.09 [23.62-48.41], 49.7 ^b	9.58 [6.45-13.22]
Lagoons	50 [28-81]	0.11 [0.05-0.13]	8.69 [4.23-10.31]	2.99 [1.45-3.54]	9.93 [6.24-13.77], 14.1 ^b	2.71 [1.70-3.76]
Fjords	-66 [-96- -24]	0.003 [0.002- 0.008]	0.26 [0.15-0.63]	0.09 [0.05-0.22]	16.33 [11.77-20.56], 30.5 ^b	4.46 [3.21-5.61]
Estuaries	111 [73-170]	0.25 [0.07-0.46]	19.95 [5.56-37.59]	6.85 [1.91-12.92]	61.34 [41.39-93.81], 94.4^b	16.75 [11.30-25.61]
Mangroves	-359 [-434- -333]	0.34 [0.21-0.50]	27.29 [16.75-40.57]	9.38 [5.76-13.94]	8.85 [4.36-19.30]	2.42 [1.19-5.27]
Salt marshes	-50 [-59- -41]	0.26 [0.14-0.36]	20.71 [11.43-28.87]	7.12 [3.93-9.92]	2.06 [-0.83-6.08]	0.56 [-0.23-1.66]
Seagrasses	-192 [-354- -53]	0.17 [0.09-0.21]	13.96 [7.17-17.20]	4.80 [2.46-5.91]	-4.56 [-5.98- -3.39]	-1.25 [-1.63- -0.93]
Coastal vegetation	-601 [-774- -426]	0.77 [0.47-1.41]	61.96 [38.13- 114.64]	21.30 [13.10- 39.39]	6.35 [0.70-18.31]	1.73 [0.19-5.00]
Estuaries + coastal vegetation	-489 [-701- -256]	1.01 [0.54-1.87]	81.90 [43.68-152]	28.14 [15.01- 52.31]	67.69 [42.10-112]	18.48 [11.49-30.61]

a) The GWP for N₂O fluxes is 273 for both 20-year and 100-year time periodsb) Based on the mechanistic model by Maavara et al.²⁵. Most of the differences in estuarine N₂O emissions between the modelled and data-driven approaches arise from North America, where modeled emissions exceed observation-based emissions by 8.6 Gg N₂O yr⁻¹. In North and South America, Russia, and Australasia, modelled emissions from tidal systems and deltas are generally lower than data-driven estimates, while North America, Russia, South Asia, and Australasia lagoon estimates are smaller in the model output. Fjord estimates represent the largest relative difference between modelled and data-driven estimates.

Table 2. Regional coastal CO₂-equivalent GHG fluxes. Median [Q1-Q3] GHG fluxes from estuaries and coastal vegetation as CO₂-equivalents (CO₂e) using the GWP₂₀ and GWP₁₀₀. Negative values indicate net uptake of GHGs from the atmosphere and positive values indicate net release of GHGs to the atmosphere.

Region	Estuaries		Coastal vegetation		Estuaries + coastal vegetation	
	Tg CO ₂ e yr ⁻¹ (GWP ₂₀)	Tg CO ₂ e yr ⁻¹ (GWP ₁₀₀)	Tg CO ₂ e yr ⁻¹ (GWP ₂₀)	Tg CO ₂ e yr ⁻¹ (GWP ₁₀₀)	Tg CO ₂ e yr ⁻¹ (GWP ₂₀)	Tg CO ₂ e yr ⁻¹ (GWP ₁₀₀)
North America	-20.0 [-33.6- -5.8]	-25.6 [-33.9- -12.0]	-89.1 [-123.7- -42.4]	-101.8 [-131.0- -64.2]	-109.0 [-157.3- -48.2]	-127.4 [-165.0- -76.2]
South America	13.3 [7.7-26.2]	11.6 [6.6-22.8]	-48.5 [-66.1- -26.7]	-51.1 [-66.1- -32.7]	-35.1 [-58.4- -0.5]	-39.5 [-59.5- -9.9]
Europe	31.3 [28.5-36.3]	30.5 [27.9-34.9]	-14.5 [-19.5- -5.7]	-15.1 [-19.9- -6.4]	16.8 [9.0-30.6]	15.5 [8.1-28.5]
Africa	25.2 [13.4-45.1]	23.4 [13.4-37.4]	-110.4 [-143.3- -56.2]	-115.9 [-147.1- -73.1]	-85.2 [-129.9- -11.0]	-92.5 [-133.7- -35.7]
Russia	30.4 [25.7-41.9]	29.3 [25.4-38.3]	-3.7 [-6.0- -1.1]	-5.2 [-7.0- -3.0]	26.7 [19.7-40.8]	24.1 [18.4-35.3]
West Asia	1.0 [0.9-1.3]	1.0 [0.9-1.2]	-22.8 [-29.3- -12.6]	-23.5 [-29.8- -15.0]	-21.8 [-28.4- -11.3]	-22.5 [-28.9- -13.8]
East Asia	7.6 [6.2-10.4]	7.2 [6.0-9.8]	-10.0 [-17.9- -2.9]	-15.0 [-21.8- -9.7]	-2.4 [-11.7-7.5]	-7.8 [-15.7-0.1]
South Asia	12.6 [10.6-13.9]	12.5 [10.5-13.8]	-21.5 [-30.7- -8.3]	-24.2 [-31.9- -13.4]	-8.9 [-20.1-5.6]	-11.7 [-21.4-0.4]
Southeast Asia	12.5 [8.0-21.4]	12.3 [7.8-21.2]	-164.8 [-229.1- -122.7]]	-168.0 [-231.4- -126.9]	-152.3 [-221.1- -101.3]	-155.7 [-223.7- -105.8]
Australasia	33.8 [22.1-42.8]	32.5 [21.4-41.4]	-51.7 [-69.6- -27.9]	-57.8 [-74.3- -37.3]	-17.9 [-47.4-14.9]	-25.3 [-52.9-4.1]
Global	147.8 [89.6-233.5]	134.7 [85.9-208.9]	-536.9 [-735.2- -306.5]	-577.5 [-760.2- -381.8]	-389.1 [-645.7- -73.0]	-442.9 [-674.3- -172.9]

Online Methods

Definitions of coastal ecosystems

Estuaries

We categorised estuaries into three major groups, following an updated version of the Dürr et al.¹ typology: 1) ‘tidal systems and deltas’, which include all open tidal systems from alluvial estuaries to tidal bays and rias as well as deltas, thus combining types I, II and V of Dürr et al.’s¹ typology; 2) ‘lagoons’, which include enclosed shallow estuarine systems with minimal tidal influence and relatively long water residence times, corresponding to type III in Dürr et al.’s¹ typology; and 3) ‘fjords’, which include all fjords with typical U-shaped valleys created by glaciers as well as other coastal glacial depression such as fjärds, defined as type IV in Dürr et al.¹. It is currently difficult to systematically define the landward boundary of estuaries, but the surface area (tidal river) remains small (10%) compared to the entire estuary area². Therefore, in our synthesis, we exclude the upper tidal river because of insufficient data for GHG fluxes and unknown surface area.

Coastal vegetation

We refer to coastal vegetation as near-shore coastal vegetated ecosystems with salinity > 0.5 that comprise emergent tidal 1) mangrove forests, 2) salt marshes, and 3) submergent seagrass meadows. We limit our analysis to these classical three coastal ‘blue carbon’ ecosystems because macroalgae have not been globally mapped. We exclude freshwater tidal marshes (< 0.5 salinity) and areas of unvegetated coastal habitats such as sandy sediments and bare rocks. These are not well mapped but may make up a significant fraction of tidal wetlands (25–28% in the contiguous United States³). We follow the definitions and areal distributions provided in Bunting et al.⁴ for mangrove forests, Mcowen et al.⁵ for salt marshes, and United Nations Environment Programme World Conservation Monitoring Centre (UNEP-WCMC) and Short⁶ for seagrasses. Briefly, areal mangrove forest coverage mainly captures mangrove tree canopy and potentially small creeks between trees but may underestimate non-terrestrial parts of mangrove ecosystems. Salt marshes are defined as the upper, vegetated portion of inter-tidal mudflats, lying approximately between mean high water neap tides and mean high water spring tides. The halophytic shrubs and grasses are adapted to regular or occasional flooding by tides⁵. Seagrass meadows can be fully submerged over the tidal cycle or partially exposed during low tide. Because seagrasses are mostly submerged, habitat mapping is challenging, and the global distribution remains uncertain^{6–8}. Also, seagrass and estuary surface areas may overlap, which

would require matching shape files/masks of estuary maps (not available globally) with seagrass maps (available, see UNEP-WCMC Short⁶).

Global and regional surface areas

Estuary surface areas

Despite the recent improvement of remote sensing imagery and Geographic Information Systems (GIS) which have helped better constrain the spatial distribution of ecosystems such as coastal wetlands in recent years^{4,9}, the only available estimates of global estuarine surface areas rely on the upscaling of empirical relations rather than a systematic and exhaustive cartography. Woodwell et al.¹⁰ derived a ratio of estuarine surface area per length of coast from a US-based survey and applied it to the entire global coastline, leading to a global estimate of $1.4 \times 10^6 \text{ km}^2$ including the Baltic Sea. This estimate was later revised by Dürr et al.¹ using a type-specific approach, which brought the estimate down to $\sim 10^6 \text{ km}^2$. This later estimate is still largely uncertain because it was only calibrated on limited sections of the world (US, UK, Australia, and Sweden) and these numbers already revealed that the so-call Woodwell ratio varies significantly from one region to the other. Furthermore, the spatial resolution of the Dürr et al.¹ typology of 0.5 degree assumed that only one type of estuary could be found within stretches of several tens of kms.

The estuarine surface areas used in this study were calculated using a novel regionalized approach that combines available national databases and an extrapolation method that derives the total estuarine surface area of a region from the surface areas of its largest systems². Using a well-established global coastal segmentation comprising 45 regions (MARgins and CATchment Segmentation, (MARCATS)¹¹), a surface area was determined for each estuary type (tidal systems and deltas, lagoons, or fjords) in each region. Wherever exhaustive regional or national databases were available and covered an entire MARCATS segment (i.e., Australia, New Zealand, and all lagoons surrounding the Mediterranean Sea), the type-specific surface areas were extracted from these databases by assigning each identified system to a given type. In other regions, the surface areas were extrapolated from the 5 to 10 largest systems. The extrapolation method relies on the observation that the cumulative estuarine surface area expressed as a function of the number of estuaries ranked by decreasing size within a sufficiently large stretch of coastline can be fitted by an equation of the form $S = (a * N) / (b + N)$ with S being the total estuarine surface area (in km^2), N , the number of estuaries and a and b dimensionless calibration coefficients. Using several extensive national estuarine databases (Australia, New Zealand, United States), it was shown that fitting the parameters of this generic

formula using only the 10 largest estuaries of a given region generally allows predicting the total cumulative surface area of the region with a 9 % accuracy. This uncertainty due to extrapolation is complemented by an uncertainty associated with the accuracy in estimating the surface areas of the individual systems used to perform the calculations and which range from 4 to 15% depending on the estuarine type. Within each MARCATS, the surface areas of the 10 largest systems of each estuarine type were gathered from national databases (United Kingdom, Mexico, United States, Australia, South Africa, South Korea), regional surveys (FAO, UNESCO), global databases (Sea Around Us) or calculated individually using GIS. Those data were then sorted and fitted using the equation described above to derive the estuarine surface area for each MARCATS and each estuarine type, and finally summed to obtain the area for each of the ten RECCAP2 regions. For further details, see Laruelle et al.².

Coastal vegetation surface areas

For all three coastal vegetation types, we segmented the vegetation area given as a global collection of polygons⁴⁻⁶ into the larger MARCATS regions¹¹ using the following approach: The MARCATS regions were first converted from the raster format to polygons using the python package *rasterio*¹². To find the area of each coastal vegetation type within a given MARCATS region we first dissolved overlapping individual polygons to avoid overestimation of the vegetation area. We found the union of each polygon and the larger MARCATS region and recalculated the area using the EPSG:6933 projection, using the python package *geopandas*¹³, and finally summed these values. The same process was repeated for each large-scale MARCATS region and vegetation type individually. The available shapefiles for MARCATS regions were converted from gridded outputs to polygons using *rasterio*¹². Using *geopandas* for each region, we dissolved overlapping polygons and calculated the area of each polygon within the region using the EPSG:6933 projection, and finally summed the area for each of the ten RECCAP2 regions.

Estuary GHG fluxes

We calculated estuary water-air fluxes of CO₂, CH₄ and N₂O based on data from peer-reviewed publications until the end of 2020. For each site/study location (> 10 km apart), we averaged spatial and seasonal variation to a single water-air flux density, resulting in 204 sites for CO₂, 157 sites for CH₄ and 123 sites for N₂O, globally, which are 20%, 21% and 85% more sites compared to previous global syntheses for CO₂ (Chen et al.¹⁴), CH₄ (Rosentreter et al.¹⁵), and N₂O (Murray et al.¹⁶), respectively. Each site/flux density was then distributed following the

ten RECCAP2 regions using lat/long coordinates provided in the original studies or from Google Earth based on the study site description. Sites were categorised as either ‘tidal systems and deltas’, ‘lagoons’, or ‘fjords’ based on the authors’ characterisation of their study site. In systems for which the site description was ambiguous or not detailed enough, the type was assigned following the hierarchical steps for estuarine type determination provided by Dürr et al.¹ which are based on hydrological, lithological, and morphological criteria. Estuary CO₂ and CH₄ emissions have not been modelled at global scales because of the lack of an existing spatially explicit global estuarine model designed to perform such a task. However, we supplemented the literature-derived empirical estuarine estimates of N₂O emissions with results from the spatially explicit global model from Maavara et al.¹⁷. These authors used a stochastic-mechanistic model representing generalized nitrogen dynamics for water body types directly connected to river networks worldwide to extract relationships predicting N₂O emissions from water residence times and total nitrogen (TN) yields (i.e., area-normalized loads) delivered to each estuary. The global TN loads were calculated using an approach inspired by Global-NEWS models¹⁸, and spatially routed nitrogen through an inland water network joined to the estuaries accounted for in Dürr et al.¹. Emissions factors were calculated using scenarios that reflect existing literature assumptions and datasets. The model was aggregated at a spatial resolution of 0.5 degrees, which is the same used by Dürr et al.¹ for their estuarine typology. Each watershed thus was assigned an estuarine type based on the type of the coastal cell in which the mouth of the watershed was located. Complete model details are available in Maavara et al.¹⁷.

Coastal vegetation GHG fluxes

Our literature search until the end of 2020 resulted in 37 sites for CO₂, 162 sites for CH₄ and 55 sites for N₂O in coastal vegetation, which are 15% and 42% more sites compared to previous global syntheses of coastal wetlands for CH₄ (Rosentreter et al.¹⁵) and N₂O (Murray et al.¹⁶), respectively. This is the first global synthesis for CO₂ that uses only long-term eddy-covariance measurements (including some unpublished data) in coastal vegetation. For coastal vegetation CO₂ fluxes, we exclude chamber measurements as they do not provide information on CO₂ exchange at the ecosystem scale. Although EC towers are still relatively rare in coastal vegetation, this method provides robust high-resolution long-term monthly, seasonal, and often annual data of net ecosystem exchange. EC measurements of CH₄ and N₂O are extremely rare in coastal wetlands. Therefore, we combined the few existing EC data with water-air, sediment-air, plant-air, and sediment-water CH₄ or N₂O fluxes where available.

CO₂-equivalent fluxes

For the purpose of directly comparing the relative radiative forcing effects of CO₂, CH₄, and N₂O to one another, we express GHG fluxes as CO₂-equivalents for the 20-year and 100-year time horizons using the global warming potential (GWP₂₀ and GWP₁₀₀) reported in the most recent IPCC assessment report¹⁹. Accordingly, over a 20-year time period, which is important for climate policies based on shorter timescales, 1 kg of CH₄ and N₂O have the same global warming potential as 81.2 kg or 273 kg of CO₂, respectively. Over a 100-year time period, 1 kg of CH₄ or N₂O have the same global warming potential as 27.9 kg or 273 kg of CO₂, respectively. The net contemporary GHG balance for a given region, ecosystem, and time horizon is the sum of the CO₂-equivalents over the three gases.

Data analyses and upscaling method

Data processing and statistical analyses were performed in R software²⁰. A non-parametric bootstrapping method using the package *boot* in R was applied to resample flux densities for each of the 3 gases in each of the 6 ecosystems (3 estuary types and 3 coastal vegetation types) and in each of the 10 RECCAP2 regions (Supplementary Figure S3). The bootstrapping method used 1,000 iterations of the median of samples to produce a smoothed distribution of flux densities, and to generate a full set of statistics (minimum, Q1, median, mean, Q3, maximum). Results from non-parametric bootstrapping were then multiplied by the corresponding surface area of each of the 6 ecosystem types in each of the 10 RECCAP2 regions. If an ecosystem type had less than three sites in a region, we applied the global statistics of this type in this region.

Uncertainty analysis

Uncertainties associated with flux densities were derived from the bootstrapping method that generated a full set of statistics including the first (Q1) and third (Q3) quartiles of the datasets. For estuarine surface areas, the normality of the distribution was successfully tested and allowed deriving upper and lower 95% confidence intervals (c.i.) as well as the first (Q1) and third (Q3) quartiles from the standard deviation². Global mangrove forest has been successfully mapped with an overall accuracy of 99% likelihood that the true value is between 93.6-94.5%⁴. The global extent of salt marshes is relatively uncertain with recent global estimates ranging from 55,000⁵ to 90,800 km²⁹. Submerged seagrasses are challenging to map and current global estimates are highly uncertain. The most recent and continuously updated global seagrass

mapping effort by UNEP-WCMC and Short⁶ does not estimate uncertainty. Here, we assume an area per region uncertainty of 5%, 10%, and 20% for mangroves, salt marshes, and seagrasses, respectively, noting that these uncertainties could be significantly larger for the latter two types of coastal vegetation. We then combined the respective uncertainties of GHG flux densities with uncertainties of surface area of either estuaries or coastal vegetation using the ‘Root Sum of the Squares’ method, which calculates the square-root of the linear sum of the squared standard uncertainty components, treating the uncertainty contributors as statistically independent. We present the combined uncertainties of Q1 and Q3 in accordance with the median (Q2) in the main article, because this statistical set represents the most appropriate measure of the non-normally distributed GHG fluxes.

Methods References

1. Dürr, H. H. *et al.* Worldwide typology of nearshore coastal systems: defining the estuarine filter of river inputs to the oceans. *Estuaries and Coasts* **34**, 441–458 (2011).
2. Laruelle, G. G., Rosentreter, J. A., Regnier P. Extrapolation based regionalized re-evaluation of the global estuarine surface area. (in prep.).
3. Hinson, A. L. *et al.* The spatial distribution of soil organic carbon in tidal wetland soils of the continental United States. *Glob. Chang. Biol.* **23**, 5468–5480 (2017).
4. Bunting, P. *et al.* The Global Mangrove Watch—A New 2010 Global Baseline of Mangrove Extent. *Remote Sens.* **10**, 1669 (2018).
5. Mcowen, C. *et al.* A global map of saltmarshes. *Biodivers. Data J.* **5**, e11764 (2017).
6. UNEP-WCMC, Short FT (2017). Global distribution of seagrasses (version 6.0). Sixth update to the data layer used in Green and Short (2003). Cambridge (UK): UN Environment World Conservation Monitoring Centre. URL: <http://data.unepwcmc.org/datasets/7>
7. Duarte, C. M. Reviews and syntheses: Hidden forests, the role of vegetated coastal habitats in the ocean carbon budget. *Biogeosciences* **14**, 301–310 (2017).
8. Jayatilake, D. R. M. & Costello, M. J. A modelled global distribution of the seagrass biome. *Biol. Conserv.* **226**, 120–126 (2018).
9. Murray, N. J. *et al.* High-resolution mapping of losses and gains of Earth’s tidal wetlands. *Science* **376**, 744–749 (2022).
10. Woodwell, G. M., Rich, P. H. & Hall, C. A. S. Carbon in estuaries. in *Carbon and the Biosphere* (eds. Woodwell, G. M. & Pecan, E. V) 221–240 (Technical Information Center, U.S. Atomic Energy Commission, National Technical Information Service, 1973).
11. Laruelle, G. G. *et al.* Global multi-scale segmentation of continental and coastal waters from the watersheds to the continental margins. *Hydrol. Earth Syst. Sci.* **17**, 2029–2051 (2013).

12. Gillies, S., Ward, B., & Petersen, A. S. (2013). Rasterio: Geospatial raster I/O for Python programmers. URL <https://github.com/mapbox/rasterio>
13. Kelsey Jordahl, Joris Van den Bossche, Martin Fleischmann, Jacob Wasserman, James McBride, Jeffrey Gerard, Jeff Tratner, Matthew Perry, Adrian Garcia Badaracco, Carson Farmer, Geir Arne Hjelle, Alan D. Snow, Micah Cochran, Sean Gillies, Lucas Culbertson, Matt Bartos, Nick Eubank, maxalbert, Aleksey Bilogur, ... François Leblanc. (2020). *geopandas/geopandas: v0.8.1 (v0.8.1)*. Zenodo. <https://doi.org/10.5281/zenodo.3946761>
14. Chen, C. T. A. *et al.* Air-sea exchanges of CO₂ in the world's coastal seas. *Biogeosciences* **10**, 6509–6544 (2013).
15. Rosentreter, J. A. *et al.* Half of global methane emissions come from highly variable aquatic ecosystem sources. *Nat. Geosci.* **14**, 225–230 (2021).
16. Murray, R. H., Emler, D. V. & Eyre, B. D. Nitrous oxide fluxes in estuarine environments: response to global change. *Glob. Chang. Biol.* **21**, 3219–3245 (2015).
17. Maavara, T. *et al.* Nitrous oxide emissions from inland waters: Are IPCC estimates too high? *Glob. Chang. Biol.* **25**, 473–488 (2019).
18. Mayorga, E. *et al.* Global Nutrient Export from WaterSheds 2 (NEWS 2): Model development and implementation. *Environ. Model. Softw.* **25**, 837–853 (2010).
19. IPCC, I. *Climate Change 2021: The Physical Science Basis. Contribution of Working Group I to the Sixth Assessment Report of the Intergovernmental Panel on Climate Change.* (2021) doi:10.1017/9781009157896.
20. R Core Team (2020). R: A language and environment for statistical computing. R Foundation for Statistical Computing, Vienna, Austria. URL <https://www.R-project.org/>. (2020).

Supplementary Material

Manuscript title: Coastal vegetation and estuaries collectively reduce global warming

Rosentreter et al.

Supplementary Figures

Content:

Figure S1: Regional and global surface areas of coastal vegetation

Figure S2: Bootstrapping approach

Figure S3 Greenhouse gas study site locations in estuaries and coastal vegetation

Supplementary Tables

Content:

Table S1: Previous global estimates of estuary and coastal vegetation CO₂ fluxes

Table S2: Previous global estimates of estuary and coastal vegetation CH₄ fluxes

Table S3: Previous global estimates of estuary and coastal vegetation N₂O fluxes

Table S4: Surface areas in estuaries and coastal vegetation

Table S5: CO₂ flux rates in estuaries and coastal vegetation

Table S6: CH₄ flux rates in estuaries and coastal vegetation

Table S7: N₂O flux rates in estuaries and coastal vegetation

Table S8: Number of sites of GHG flux studies in estuaries and coastal vegetation

Figure S1: Regional and global surface areas of coastal vegetation

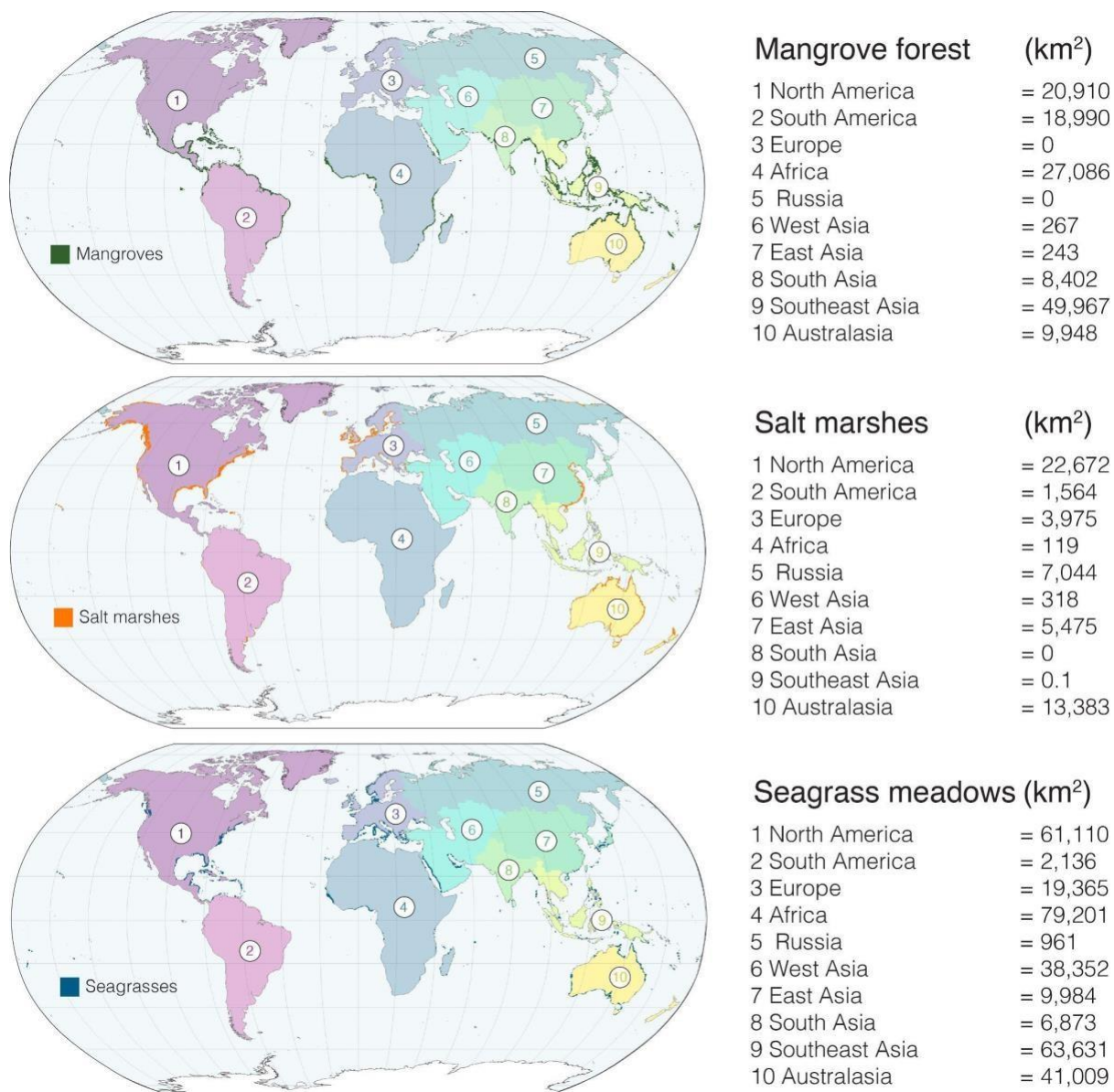


Figure caption: Map showing the ten RECCAP2 regions and global coastal vegetation distribution of mangrove forest, salt marshes, and seagrass meadows. To the right: regional surface areas (km²) of mangroves, salt marshes, and seagrasses in the ten world regions.

Figure S2: Bootstrapping approach

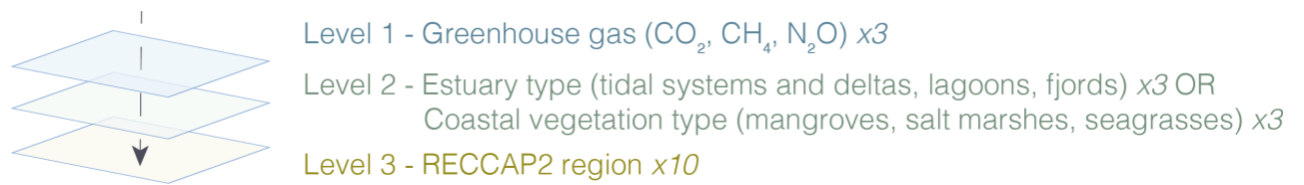


Figure caption: Bootstrapping was applied to randomly resample flux densities of the three greenhouse gases (level 1) for each estuary or coastal vegetation types (level 2) for each of the 10 RECCAP2 regions (level 3) before upscaling to specific surface areas.

Figure S3 Greenhouse gas study site locations in estuaries and coastal vegetation

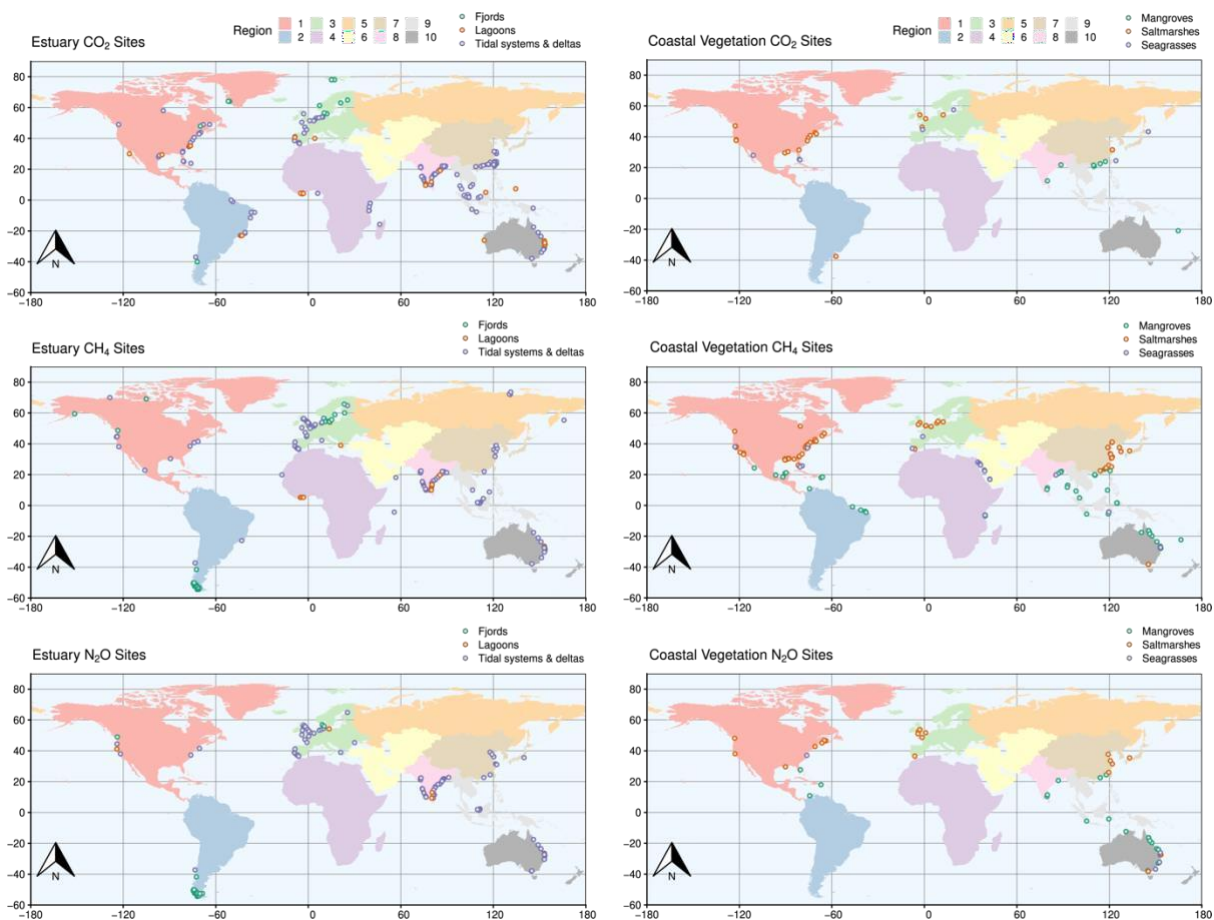


Figure caption: Map showing locations of CO₂, CH₄, and N₂O flux studies in the ten RECCAP2 regions in estuaries (left side): tidal systems and deltas, lagoons, and fjords, and coastal vegetation (right side): in mangroves, salt marshes, and seagrasses, from peer-reviewed publications until the end of 2020. Exact number of study sites can be found in Supplementary Table S8.

Table S1: Previous global estimates of estuary and coastal vegetation CO₂ fluxes

System	CO ₂ flux (Pg CO ₂ yr ⁻¹)	n = sites	Surface area (x 10 ⁶ km ²)	Surface area reference	Global estimate reference	Notes
Tidal wetlands	2.82-11.66				Duarte et al. (2005) ¹	Net ecosystem production (NEP)
Salt marshes and mangroves	0.51				Duarte (2017) ²	Net primary production (NPP)
Seagrasses	1.47				Duarte (2017) ²	Net primary production (NPP)
Mangroves	0.16	7	0.2		Borges et al. (2003) ³	Water-air flux only
Mangroves	0.15 ± 0.14		0.16	FAO (2003) ⁴	Bouillon et al. (2008) ⁵	Water-air flux only, mean ± SE
Mangroves	0.16		0.150791	Spalding et al. (2010) ⁶	Alongi and Mukhopadhyay (2015) ⁷	Water-air flux only
Mangroves	0.17		0.146	FAO (2003) ⁴	Koné and Borges (2008) ⁸	Water-air flux only
Mangroves	0.095		0.138	Giri et al. (2011) ⁹	Alongi (2014) ¹⁰	Water-air flux only
Mangroves	0.13 ± 0.02	36	0.137760	Giri et al. (2011) ⁹	Rosentreter et al. (2018) ¹¹	Water-air flux only, mean ± SE
Tidal wetlands	-0.55				Cai (2011) ¹²	
Tidal wetlands	-1.65 ± 1.65		0.4		Bauer et al. (2013) ¹³	
Tidal wetlands	-1.1 & -0.55				Regnier et al. (2013) ¹⁴	2 estimates (1750 & 2010),
Salt marshes and mangroves	-0.66 ± 0.29				Regnier et al. (2022) ¹⁵	2 sigma error
Submerged vegetation in estuaries	-0.18 ± 0.15				Regnier et al. (2022) ¹⁵	2 sigma error
Estuaries	2.2	19	1.4	Woodwell et al. (1973) ¹⁶	Abril and Borges (2004) ¹⁷	Including intertidal areas
Estuaries	1.6	16	0.94	Woodwell et al. (1973) ¹⁶	Borges (2005) ¹⁸	Excluding intertidal areas

Estuaries	1.2	16	0.94	Woodwell et al. (1973) ¹⁶	Borges et al. (2005) ¹⁹	Excluding intertidal areas
Estuaries	1.3	32	0.943	Woodwell et al. (1973) ¹⁶	Chen and Borges (2009) ²⁰	Excluding intertidal areas
Estuaries	0.98 ± 0.83	60	1.067	Dürr et al. (2011) ²¹	Laruelle et al. (2010) ²²	
Estuaries	0.92		1.05	Dürr et al. (2011) ²¹	Cai (2011) ¹²	
Estuaries	0.98 ± 0.83	62	1.067	Dürr et al. (2011) ²¹	Borges and Abril (2011) ²³	
Estuaries	0.95	106	1.07	Dürr et al. (2011) ²¹	Chen et al. (2012) ²⁴	Area-weighted fluxes
Estuaries	0.55	161	1.0	Laruelle et al. (2013)	Laruelle et al. (2013) ²⁵	68 of the sites use a relationship with NEM, area-weighted fluxes
Estuaries	0.92 ± 0.92		1.1	Dürr et al. (2011) ²¹	Regnier et al. (2013) ¹⁴	
Estuaries	0.92 ± 0.92		1.1	Dürr et al. (2011) ²¹	Bauer et al. (2013) ¹³	95% confidence range
Estuaries	0.4	165	1.0	Laruelle et al. (2013)	Chen et al. (2013) ²⁶	
Estuaries	0.55				Regnier et al. (2022) ¹⁵	Based on Laruelle et al. (2013)

Table S2: Previous global estimates of estuary and coastal vegetation CH₄ fluxes

System	CH ₄ flux (Tg CH ₄ yr ⁻¹)	n = sites	Surface area (x 10 ⁶ km ²)	Surface area reference	Global estimate reference	Notes
Mangroves	0.03-1.7	23	0.137760	Giri et al. (2011) ⁹	Rosentreter et al. (2018) ²⁷	Water-air and sediment-air fluxes, upscaled based on arithmetic means, does not report medians
Mangroves	3.68-4		0.137760 - 0.152361	Mcleod et al. (2011) ²⁸	Al-Haj and Fulweiler (2020) ²⁹	Upscaled based on arithmetic means
Mangroves	0.21 ± 0.91	59	0.137600	Bunting et al. (2018) ³⁰	Rosentreter et al. (2021) ³¹	Median (± 95% C.I.)
Salt marshes	1.1		0.054951	Mcowen et al. (2017) ³²	Al-Haj and Fulweiler (2020) ²⁹	Upscaled based on arithmetic means
Salt marshes	0.18 ± 1.51	60	0.054951	Mcowen et al. (2017) ³²	Rosentreter et al. (2021) ³¹	Median (± 95% C.I.)
Seagrasses	0.09-2.7		0.15-4.32	Duarte (2017) ²	Garcias-Bonet and Duarte (2017) ³³	Flux (n=13) per species
Seagrasses	0.5-1.0		0.788-1.6468	Jayathilake and Costello (2018) ³⁴ ; Davidson and Finlayson (2019) ³⁵	Al-Haj and Fulweiler (2020) ²⁹	Upscaled based on arithmetic means
Seagrasses	0.13 ± 0.09	18	0.266582	Mckenzie et al. (2020) ³⁶	Rosentreter et al. (2021) ³¹	Median (± 95% C.I.)
Estuaries	0.8-1.32		1.4	Woodwell et al. (1973) ¹⁶	Bange et al. (1994) ³⁷	Literature compilation, applied global exchange coefficient

Estuaries	0.9-1.7		1.4	Woodwell et al. (1973) ¹⁶	Upstill-Goddard et al. (2000) ³⁸	Upscaled based on mean river CH ₄ concentration and 90% estuarine CH ₄ removal
Estuaries	1.8-3.0	8	1.4	Woodwell et al. (1973) ¹⁶	Middelburg et al. (2002) ³⁹	Literature compilation, applied global exchange coefficient
Estuaries	6.6	32	1.1	Dürr et al. (2011) ²¹	Borges and Abril (2011) ²³	Estuaries and some coastal wetlands combined, upscaled based on arithmetic means
Estuaries	0.23 ± 0.29	124	1.02	Woodwell et al. (1973) ¹⁶ ; Dürr et al. (2011) ²¹	Rosentreter et al. (2021) ³¹	Median (± 95% C.I.)

Table S3: Previous global estimates of estuary and coastal vegetation N₂O fluxes

System	N ₂ O flux (Tg N ₂ O yr ⁻¹)	n = sites	Surface area (x 10 ⁶ km ²)	Surface area reference	Global estimate reference	Notes
Mangroves	0.014-0.56	4	0.18	Spalding (1997) ⁴⁰	Corredor et al. (1999) ⁴¹	Seasonal study, extrapolation based on four sites
Mangroves	0.12	1	0.56	Borges et al. (2003) ³ ; Selvam (2003) ⁴²	Barnes et al. (2006) ⁴³	Seasonal study, extrapolation based on one site
Mangroves	0.11	1	0.56		Chauhan et al. (2008) ⁴⁴	Seasonal study, extrapolation based on one site
Mangroves	0.05	16	0.15	Pendleton et al. (2012) ⁴⁵	Murray et al. (2015) ⁴⁶	Literature compilation of fluxes, median
Salt marshes	0.006	15	0.05	Pendleton et al. (2012) ⁴⁵	Murray et al. (2015) ⁴⁶	Literature compilation of fluxes, median
Seagrasses	0.046	9	0.3	Pendleton et al. (2012) ⁴⁵	Murray et al. (2015) ⁴⁶	Literature compilation, based on N ₂ O/N ratios, median
Estuaries	0.22	1	1.4	Woodwell (1980) ⁴⁷	Law et al. (1992) ⁴⁸	Seasonal study, extrapolation based on one estuary
Estuaries	3.7-5.7	11	1.4	Woodwell (1980) ⁴⁷	Bange et al. (1996) ⁴⁹	Literature compilation, applied global exchange coefficient
Estuaries	0.11-1.08				Seitzinger and Kroeze (1998) ⁵⁰	Derived from NEWS model, N model
Estuaries	0.71	1	1.4	Woodwell (1980) ⁴⁷	Robinson et al. (1998) ⁵¹	Seasonal study, extrapolation based on one estuary
Estuaries	1.5	1	1.4	Whittaker and Likens (1975) ⁵²	De Wilde and de Bie (2000) ⁵³	Seasonal study, extrapolation based on one estuary
Estuaries	0.39	1			Kroeze et al. (2005) ⁵⁴	Derived from NEWS model
Estuaries	0.16-0.94				Kroeze et al. (2010) ⁵⁵	Derived from NEWS model

Estuaries	0.36 (0.20-0.69)	22	1.25	Woodwell (1980) ⁴⁷ ; Dürr et al. (2011) ²¹	Murray et al. (2015) ⁴⁶	Literature compilation of fluxes, median, estuarine open waters
Estuaries	0.09-0.24		1.1	Woodwell et al. (1973) ¹⁶ ; Dürr et al. (2011) ²¹	Maavara et al. (2019) ⁵⁶	Derived from NEWS model
Estuaries	0.4		1.25	Murray et al. (2015) ⁴⁶	Zheng et al. (2022) ⁵⁷	Literature compilation, statistical mean of flux data

Table S4: Surface areas in estuaries and coastal vegetation

Regional and global estuary and coastal vegetation surface areas in km². NA indicates that estuary or coastal vegetation type is absent in this region. The estuarine surface area uncertainty is given as ± 2 sigma (Laruelle et al.⁵⁸). For mangroves, salt marshes, and seagrasses no regional uncertainty measures are available from global maps, therefore we assume 5%, 10%, and 20%, respectively, per RECCAP2 region for our uncertainty analysis (*see Methods*).

Regions	Tidal systems/deltas	Lagoons	Fjords	Mangroves	Salt marshes	Seagrasses
North America	67,197 \pm 19,345	68,044 \pm 9,627	193,644 \pm 21,404	20,910 \pm 1,045	22,672 \pm 2,267	61,110 \pm 12,222
South America	57,946 \pm 14,436	31,332 \pm 5,349	21,988 \pm 4,113	18,990 \pm 950	1,564 \pm 156	2,136 \pm 427
Europe	14,287 \pm 3,435	14,452 \pm 3,154	24,306 \pm 3,593	NA	3,975 \pm 397	19,365 \pm 3,873
Africa	22,494 \pm 5,252	14,688 \pm 2,214	NA	27,086 \pm 1,354	119 \pm 12	79,201 \pm 15,840
Russia	53,548 \pm 12,778	20,200 \pm 2,483	18,182 \pm 3,254	NA	7,044 \pm 704	961 \pm 192
West Asia	1,395 \pm 630	1,070 \pm 179	NA	267 \pm 13	318 \pm 32	38,352 \pm 7,670
East Asia	10,421 \pm 3,353	2,137 \pm 924	NA	243 \pm 12	5,475 \pm 547	9,984 \pm 1,997
South Asia	22,750 \pm 7,903	5,421 \pm 1,228	NA	8,402 \pm 420	NA	6,873 \pm 1,375
Southeast Asia	19,878 \pm 6,895	2,542 \pm 236	NA	49,967 \pm 2,498	NA	63,631 \pm 12,726
Australasia	25,041 \pm 6,344	20,060 \pm 780	779 \pm 18	9,948 \pm 497	13,383 \pm 1,338	41,009 \pm 8,202
Global (km²)	294,956\pm 30,780	179,946\pm 12,056	258,899\pm 22,328	135,812\pm 6,790	54,550\pm 5,455	322,620\pm 64,524

Table S5: CO₂ flux densities in estuaries and coastal vegetation

Median [Q1-Q3] estuary water-air CO₂ flux densities and coastal vegetation CO₂ flux densities for each RECCAP2 region and as global total. n < 3 indicates that less than 3 sites were available in this region. NA indicates that estuary or coastal vegetation type is absent in this region. Positive values indicate a flux from the ecosystem/water to the atmosphere, negative values indicate a flux from the atmosphere to the ecosystem/water.

Region	CO ₂ (g CO ₂ m ⁻² d ⁻¹)			CO ₂ (g CO ₂ m ⁻² yr ⁻¹)		
	Tidal systems/ deltas	Lagoons	Fjords	Mangroves	Salt marshes	Seagrasses
North America	0.52 [0.43-0.65]	0.36 [0.14-0.57]	-0.81 [-1.08- -0.43]	n < 3	-741 [-777- -656]	n < 3
South America	0.60 [0.08-1.57]	n < 3	n < 3	n < 3	n < 3	n < 3
Europe	4.77 [4.52-5.76]	n < 3	0.02 [-0.48-0.42]	NA	-968 [-1,173- -359]	n < 3
Africa	1.19 [0.74-1.87]	2.22 [0.61-3.74]	NA	n < 3	n < 3	n < 3
Russia	n < 3	n < 3	n < 3	NA	n < 3	n < 3
West Asia	n < 3	n < 3	NA	n < 3	n < 3	n < 3
East Asia	1.42 [1.29-1.88]	n < 3	NA	n < 3	-2,108 [-2,328- -1,885]	n < 3
South Asia	0.53 [0.45-0.61]	4.00 [3.61-4.24]	NA	n < 3	NA	n < 3
Southeast Asia	1.38 [0.78-1.92]	n < 3	NA	-2,644 [-3,414- -2,508]	n < 3	n < 3
Australasia	2.65 [1.80-2.96]	0.95 [0.36-2.40]	n < 3	n < 3	n < 3	n < 3
Global	1.22 [1.02-1.49]	0.71 [0.57-0.95]	-0.34 [-0.61-0.10]	-2,647 [-3036- -2,508]	-777 [-1,082- -763]	-594 [-1,082- -183]

Table S6: CH₄ flux densities in estuaries and coastal vegetation

Median [Q1-Q3] estuary water-air CH₄ flux densities and coastal vegetation CH₄ flux densities for each RECCAP2 region and as global total. n < 3 indicates that less than 3 sites were available in this region. NA indicates that estuary or coastal vegetation type is absent in this region. Positive values indicate a flux from the ecosystem/water to the atmosphere, negative values indicate a flux from the atmosphere to the ecosystem/water.

Region	CH ₄ (mg CH ₄ m ⁻² d ⁻¹)			CH ₄ (mg CH ₄ m ⁻² d ⁻¹)		
	Tidal systems/ deltas	Lagoons	Fjords	Mangroves	Salt marshes	Seagrasses
North America	2.90 [2.90-5.14]	n < 3	0.03 [0.01-0.05]	18.48 [13.77-24.50]	9.71 [5.41-15.60]	0.75 [0.45-0.80]
South America	n < 3	n < 3	0.04 [0.03-0.08]	6.10 [0.03-13.68]	n < 3	n < 3
Europe	1.35 [1.05-1.78]	n < 3	0.09 [0.06-0.32]	NA	0.62 [0.48-0.99]	n < 3
Africa	n < 3	5.25 [1.25-5.41]	NA	n < 3	n < 3	n < 3
Russia	0.55 [0.17-1.77]	n < 3	n < 3	NA	n < 3	n < 3
West Asia	n < 3	n < 3	NA	0.08 [0.05-1.13]	n < 3	0.88 [0.44-1.20]
East Asia	1.64 [0.91-2.37]	n < 3	NA	21.19 [13.65-26.43]	43.68 [23.64-46.47]	n < 3
South Asia	0.04 [0.01-0.04]	0.85 [0.30-2.07]	NA	15.38 [6.70-25.21]	NA	n < 3
Southeast Asia	0.43 [0.37-0.49]	n < 3	NA	1.37 [1.23-2.00]	n < 3	n < 3
Australasia	1.53 [1.17-1.83]	n < 3	n < 3	5.03 [3.42-7.24]	n < 3	3.02 [0.22-3.02]
Global	0.77 [0.67-0.85]	1.32 [0.77-1.54]	0.04 [0.03-0.06]	6.11 [4.64-7.51]	10.57 [6.23-15.36]	1.47 [1.20-1.63]

Table S7: N₂O flux densities in estuaries and coastal vegetation

Median [Q1-Q3] estuary water-air N₂O flux densities and coastal vegetation N₂O flux densities for each RECCAP2 region and as global total. n < 3 indicates that less than 3 sites were available in this region. NA indicates that estuary or coastal vegetation type is absent in this region. Positive values indicate a flux from the ecosystem/water to the atmosphere, negative values indicate a flux from the atmosphere to the ecosystem/water.

Region	N ₂ O (mg N ₂ O m ⁻² d ⁻¹)			N ₂ O (mg N ₂ O m ⁻² d ⁻¹)		
	Tidal systems/ deltas	Lagoons	Fjords	Mangroves	Salt marshes	Seagrasses
North America	0.38 [0.24-0.52]	n < 3	n < 3	n < 3	-0.03 [-0.05- -0.10]	n < 3
South America	n < 3	n < 3	0.16 [0.12-0.18]	n < 3	n < 3	n < 3
Europe	0.53 [0.43-0.65]	n < 3	n < 3	NA	0.05 [-0.48-0.53]	n < 3
Africa	n < 3	n < 3	NA	n < 3	n < 3	n < 3
Russia	n < 3	n < 3	n < 3	NA	n < 3	n < 3
West Asia	n < 3	n < 3	NA	n < 3	n < 3	n < 3
East Asia	0.99 [0.72-1.44]	n < 3	NA	6.77 [2.32-12.64]	0.64 [0.12-1.41]	n < 3
South Asia	0.01 [0.007-0.03]	0.20 [0.15-0.54]	NA	0.89 [0.62-2.60]	NA	n < 3
Southeast Asia	0.72 [0.22-1.35]	n < 3	NA	n < 3	n < 3	n < 3
Australasia	0.19 [0.18-0.20]	n < 3	n < 3	0.04 [0.02-0.05]	n < 3	-0.04 [-0.05- -0.04]
Global	0.25 [0.20-0.29]	0.15 [0.09-0.20]	0.17 [0.13-0.22]	0.13 [0.05-0.23]	0.11 [0.009-0.20]	-0.04 [-0.05- -0.03]
Model	0.46	0.22	0.32			

Table S8: Number of sites of GHG fluxes in estuaries and coastal vegetation

Ecosystem type	CO ₂	CH ₄	N ₂ O
Tidal systems/deltas	165	111	93
Lagoons	26	12	8
Fjords	13	34	22
Mangroves	9	67	27
Salt marshes	22	73	20
Seagrasses	6	22	8
Total	738		

1. Duarte, C. M., Middelburg, J. J. & Caraco, N. Major role of marine vegetation on the oceanic carbon cycle. *Biogeosciences* **2**, 1–8 (2005).
2. Duarte, C. M. Reviews and syntheses: Hidden forests, the role of vegetated coastal habitats in the ocean carbon budget. *Biogeosciences* **14**, 301–310 (2017).
3. Borges, A. V. *et al.* Atmospheric CO₂ flux from mangrove surrounding waters. *Geophys. Res. Lett.* **30**, 12–15 (2003).
4. FAO, State of the World's Forests, 151 pp., Food and Agric. Org. of the U.N., Rome. (2003).
5. Bouillon, S. *et al.* Mangrove production and carbon sinks: A revision of global budget estimates. *Global Biogeochem. Cycles* **22**, 1–12 (2008).
6. Dahdouh-Guebas, F. World Atlas of Mangroves: Mark Spalding, Mami Kainuma and Lorna Collins (eds). *Hum. Ecol.* **39**, 107–109 (2011).
7. Alongi, D. M. & Mukhopadhyay, S. K. Contribution of mangroves to coastal carbon cycling in low latitude seas. *Agric. For. Meteorol.* **213**, 266–272 (2015).
8. Koné, Y. J.-M. & Borges, A. V. Dissolved inorganic carbon dynamics in the waters surrounding forested mangroves of the Ca Mau Province (Vietnam). *Estuar. Coast. Shelf Sci.* **77**, 409–421 (2008).
9. Giri, C. *et al.* Status and distribution of mangrove forests of the world using earth observation satellite data. *Glob. Ecol. Biogeogr.* **20**, 154–159 (2011).
10. Alongi, D. M. Carbon cycling and storage in mangrove forests. *Ann. Rev. Mar. Sci.* **6**, 195–219 (2014).
11. Rosentreter, J. A., Maher, D. T., Erler, D. V., Murray, R. & Eyre, B. D. Seasonal and temporal CO₂ dynamics in three tropical mangrove creeks – A revision of global mangrove CO₂ emissions. *Geochim. Cosmochim. Acta* **222**, 729–745 (2018).
12. Cai, W.-J. Estuarine and Coastal Ocean Carbon Paradox: CO₂ Sinks or Sites of Terrestrial Carbon Incineration? *Ann. Rev. Mar. Sci.* **3**, 123–145 (2011).
13. Bauer, J. E. *et al.* The changing carbon cycle of the coastal ocean. *Nature* **504**, 61–70 (2013).
14. Regnier, P. *et al.* Anthropogenic perturbation of the carbon fluxes from land to ocean. *Nat. Geosci.* **6**, 597–607 (2013).
15. Regnier, P., Resplandy, L., Najjar, R. G. & Ciais, P. The land-to-ocean loops of the global carbon cycle. *Nature* **603**, 401–410 (2022).
16. Woodwell, G. M., Rich, P. H. & Hall, C. A. S. Carbon in estuaries. in *Carbon and the Biosphere* (eds. Woodwell, G. M. & Pecan, E. V) 221–240 (Technical Information Center, U.S. Atomic Energy Commission, National Technical Information Service, 1973).

17. Abril, G. & Borges, A. V. Carbon Dioxide and Methane Emissions from the coastal ocean. *Nat. Environ. Sci. Ser.* 187–207 (2004).
18. Borges, A. V. Do we have enough pieces of the jigsaw to integrate CO₂ fluxes in the coastal ocean? *Estuaries* **28**, 3–27 (2005).
19. Borges, A. V., Delille, B. & Frankignoulle, M. Budgeting sinks and sources of CO₂ in the coastal ocean: Diversity of ecosystems counts. *Geophys. Res. Lett.* (2005).
20. Chen, C.-T. A. & Borges, A. V. Reconciling opposing views on carbon cycling in the coastal ocean: Continental shelves as sinks and near-shore ecosystems as sources of atmospheric CO₂. *Deep Sea Res. Part II Top. Stud. Oceanogr.* **56**, 578–590 (2009).
21. Dürr, H. H. *et al.* Worldwide typology of nearshore coastal systems: defining the estuarine filter of river inputs to the oceans. *Estuaries and Coasts* **34**, 441–458 (2011).
22. Laruelle, G. G., Dürr, H. H., Slomp, C. P. & Borges, A. V. Evaluation of sinks and sources of CO₂ in the global coastal ocean using a spatially-explicit typology of estuaries and continental shelves. *Geophys. Res. Lett.* **37**, 1–6 (2010).
23. Borges, A. V. & Abril, G. Carbon Dioxide and Methane Dynamics in Estuaries. In *Treatise on Estuarine and Coastal Science* vol. 5 119–161 (Elsevier, 2011).
24. Chen, C. A., Huang, T., Fu, Y., Bai, Y. & He, X. Strong sources of CO₂ in upper estuaries become sinks of CO₂ in large river plumes. *Curr. Opin. Environ. Sustain.* **4**, 179–185 (2012).
25. Laruelle, G. G. *et al.* Global multi-scale segmentation of continental and coastal waters from the watersheds to the continental margins. *Hydrol. Earth Syst. Sci.* **17**, 2029–2051 (2013).
26. Chen, C. T. A. *et al.* Air-sea exchanges of CO₂ in the world's coastal seas. *Biogeosciences* **10**, 6509–6544 (2013).
27. Rosentreter, J. A., Maher, D. T., Erler, D. V., Murray, R. H. & Eyre, B. D. Methane emissions partially offset “blue carbon” burial in mangroves. *Sci. Adv.* **4**, eaa04985 (2018).
28. Mcleod, E. *et al.* A blueprint for blue carbon: toward an improved understanding of the role of vegetated coastal habitats in sequestering CO₂. *Front. Ecol. Environ.* **9**, 552–560 (2011).
29. Al-Haj, A. N. & Fulweiler, R. W. A synthesis of methane emissions from shallow vegetated coastal ecosystems. *Glob. Chang. Biol.* **26**, 2988–3005 (2020).
30. Bunting, P. *et al.* The Global Mangrove Watch—A New 2010 Global Baseline of Mangrove Extent. *Remote Sens.* **10**, 1669 (2018).

31. Rosentreter, J. A. *et al.* Half of global methane emissions come from highly variable aquatic ecosystem sources. *Nat. Geosci.* **14**, 225–230 (2021).
32. Mcowen, C. *et al.* A global map of saltmarshes. *Biodivers. Data J.* **5**, e11764 (2017).
33. Garcias-Bonet, N. & Duarte, C. M. Methane Production by Seagrass Ecosystems in the Red Sea. *Front. Mar. Sci.* **4**, 340 (2017).
34. Jayatilake, D. R. M. & Costello, M. J. A modelled global distribution of the seagrass biome. *Biol. Conserv.* **226**, 120–126 (2018).
35. Davidson, N. C. & Finlayson, C. M. Updating global coastal wetland areas presented in Davidson and Finlayson (2018). *Mar. Freshw. Res.* (2019) doi:10.1071/MF19010.
36. McKenzie, L. J. *et al.* The global distribution of seagrass meadows. *Environ. Res. Lett.* **15**, 074041 (2020).
37. Bange, H. W., Bartell, U. H., Rapsomanikis, S. & Andreae, M. O. Methane in the Baltic and North Seas and a reassessment of the marine emissions of methane. *Global Biogeochem. Cycles* **8**, 465–480 (1994).
38. Upstill-Goddard, R. C., Barnes, J., Frost, T. & Punshon, S. Methane in the southern North Sea: Low-salinity inputs, estuarine removal, and atmospheric flux. *Global Biogeochem. Cycles* **14**, 1205–1217 (2000).
39. Middelburg, J. J. *et al.* Methane distribution in European tidal estuaries. *Biogeochemistry* **59**, 95–119 (2002).
40. Spalding, M. D. The Global Distribution and Status of Mangrove Ecosystems. *Intracoast Netw. Int. Newsl. Coast. Manag. Spec. Ed. No. 1, Narragansett, RI*, 20–21 (1997).
41. Corredor, J. E., Morell, J. M. & Bauza, J. Atmospheric Nitrous Oxide Fluxes from Mangrove Sediments. *Mar. Pollut. Bull.* **38**, 473–478 (1999).
42. Selvam, V. Environmental classification of mangrove wetlands of India. *Curr. Sci.* **84**, 757–765 (2003).
43. Barnes, J. *et al.* Tidal dynamics and rainfall control N₂O and CH₄ emissions from a pristine mangrove creek. *Geophys. Res. Lett.* **33**, 4–9 (2006).
44. Chauhan, R., Ramanathan, A. L. & Adhya, T. K. Assessment of methane and nitrous oxide flux from mangroves along Eastern coast of India. in *Geofluids* vol. 8 321–332 (2008).
45. Pendleton, L. *et al.* Estimating Global “Blue Carbon” Emissions from Conversion and Degradation of Vegetated Coastal Ecosystems. *PLoS One* **7**, e43542 (2012).
46. Murray, R. H., Erler, D. V. & Eyre, B. D. Nitrous oxide fluxes in estuarine environments: response to global change. *Glob. Chang. Biol.* **21**, 3219–3245 (2015).

47. Woodwell, G. M. Aquatic systems as part of the biosphere. in *Fundamentals of Aquatic Ecosystems* (eds. Barnes, R. S. K. & Mann, H. H.) 201–215 (Blackwell Sci.Publ, 1980).
48. Law, C. S., Rees, A. P. & Owens, N. J. P. Nitrous Oxide: Estuarine Sources and Atmospheric Flux. *Estuar. Coast. Shelf Sci.* **35**, 301–314 (1992).
49. Bange, H. W., Rapsomanikis, S. & Andreae, M. O. Nitrous oxide in coastal waters. *Global Biogeochem. Cycles* **10**, 197–207 (1996).
50. Seitzinger, S. P. & Kroeze, C. Global distribution of nitrous oxide production and inputs in freshwater and coastal marine ecosystems. *Global Biogeochem. Cycles* **12**, 93–113 (1998).
51. Robinson, A. D., Nedwell, D. B., Harrison, R. M. & Ogilvie, B. G. Hypernutrified estuaries as sources of N₂O emission to the atmosphere: The estuary of the River Colne, Essex, UK. *Mar. Ecol. Prog. Ser.* **164**, 59–71 (1998).
52. Whittaker, R.H., Likens, G.E., 1975. The biosphere and man. In: Lieth, H., Whittaker, R.H. Eds. *Primary Production of the Biosphere*. Springer-Verlag, Berlin, pp. 305–328(1973).
53. De Wilde, H. P. J. & De Bie, M. J. M. Nitrous oxide in the Schelde estuary: Production by nitrification and emission to the atmosphere. *Mar. Chem.* **69**, 203–216(2000).
54. Kroeze, C., Dumont, E. & Seitzinger, S. P. New estimates of global emissions of N₂O from rivers and estuaries. *Environ. Sci.* **2**, 159–165 (2005).
55. Kroeze, C., Dumont, E. & Seitzinger, S. Future trends in emissions of N₂O from rivers and estuaries. *J. Integr. Environ. Sci.* **7**, 71–78 (2010).
56. Maavara, T. *et al.* Nitrous oxide emissions from inland waters: Are IPCC estimates too high? *Glob. Chang. Biol.* **25**, 473–488 (2019).
57. Zheng, Y. *et al.* Global methane and nitrous oxide emissions from inland waters and estuaries. *Glob. Chang. Biol.* 4713–4725 (2022) doi:10.1111/gcb.16233.
58. Laruelle, G. G., Rosentreter, J. A., Regnier P. Extrapolation based regionalized re-evaluation of the global estuarine surface area. (in prep.).